Transcription Factors DksA and PsrA are synergistic contributors to *L. pneumophila* virulence in *Acathamoeba castellanii* protozoa

CHRISTOPHER I. GRAHAM, TEASSA L. MACMARTIN, TIFFANY V. PENNER, JORDAN C. BECK, ANDREW J. GIERYS, GERD PREHNA, TERESA R. DE KIEVIT and ANN KAREN C. BRASSINGA†

Department of Microbiology, Faculty of Science, University of Manitoba, Winnipeg, Manitoba, Canada R3T 2N2

Running Title: Regulatory synergy of DksA and PsrA in *L. pneumophila*

†Corresponding author: Dr. Ann Karen C. Brassinga
Department of Microbiology (Fort Garry Campus)
Room 213, Buller Building
45 Chancellor's Circle
University of Manitoba
Winnipeg, MB, Canada
R3T 2N2
Phone: (204) 799-8457
E-mail: Ann.Brassinga@umanitoba.ca

Abstract

The environmental bacterium *Legionella pneumophila* is an intracellular parasite of free-living freshwater protozoa, and an opportunistic human pathogen. The *L. pneumophila* biphasic lifestyle depends on a complex regulatory network that is responsive to nutrient depletion cues to enable the switch from the vegetative replicative form (RF) to the environmentally resilient transmissive phase (TP) form. For a subset of TP-associated traits, RNA polymerase co-factor DksA cooperates with stringent response alarmone ppGpp to influence gene expression. Here we report that, through a dysfunctional DksA mutation (DksA1), a synergistic interplay was discovered between DksA and transcription regulator PsrA that contributes to virulence in *Acanthamoeba castellanii* protozoa. DksA could fully rescue an intracellular growth defect of a *dksA1* strain and vice versa, whereas PsrA overexpression could partially rescue the growth defect of *dksA1* strain. Conversely, *in trans* DksA expression fully restored the growth defect of a Δ*psrA* strain. Different phenotypes were observed *in vitro*; either DksA or DksA1 are required for extended culturability of bacterial cells in depleted broth, and altered cell morphology along with lack of pigmentation exhibited by the Δ*dksA* strain could only be rescued by DksA. Comparative structural modeling predicts that the DksA1 mutation affects coordination of a Mg^{2+} into the active site of RNAP compromising transcription efficiency. Thus, the largely overlapping and additive phenotypes presented in this study has led us to propose that PsrA assists DksA in the regulation of TP-associated traits. Additionally, *in vitro* evidence suggests that the long chain fatty chain response, one of the cues leading to stringent response activation, is mediated by PsrA together with DksA inferring a novel regulatory link to the stringent response pathway.

56 **Introduction**

57 *Legionella pneumophila*, a Gram-negative gammaproteobacterium, is commonly found in piped
58 water distribution systems where it is found as an intracellular parasite of free-living
59 bacterivorous protozoa (Rowbowtham, 1986; Steinert *et al.,* 2002; Newton *et al.,* 2010). These
60 environments are not only amenable to bacterial colonization and proliferation, but can also
61 aerosolize *Legionella*-laden water droplets that can be inhaled by susceptible individuals, thereby
62 facilitating bacterial infection of alveolar macrophages resulting in the atypical pneumonia
63 Legionnaires' disease (Newton *et al.,* 2010; Oliva *et al.,* 2018; Mondino *et al.,* 2020).

64 *L. pneumophila* is well adapted for its intracellular lifestyle in protozoa, and these
65 adaptations also enable human infection due to highly conserved eukaryotic cellular biology
66 (Newton *et al.,* 2010; Mondino *et al.,* 2020). A core driver of infection is the Dot/Icm Type IV
67 secretion system (T4SS); an apparatus that enables secretion of a diverse repertoire of ≥ 330
68 effectors into the host cytoplasm that together act to modify host cellular physiology upon uptake
69 of the bacteria (Finsel and Hilbi, 2015; Burstein *et al*., 2016; Gomez-Valero *et al.,* 2019b). Such
70 modifications include subversion of phagosome trafficking to prevent fusion of the bacteria-
71 containing phagosome with lysosomes, and conversion of the phagosome into a replicative niche
72 referred to as the *Legionella*-containing vacuole (LCV) (Tilney *et al.,* 2001; Kagan and Roy,
73 2002; Isberg *et al*., 2009). As infection progresses within a protozoan host cell, *L. pneumophila*
74 exhibits a biphasic lifecycle, alternating between a vegetative replicative phase (RP) forms found
75 primarily in the LCV, and transmissive phase (TP) forms that develop upon depletion of host-
76 derived nutrients in anticipation of bacterial release to the environment. The physiology and
77 ultrastructure of TP cells is optimized for environmental survival and resistance to stress, with
78 expressed virulence factors enabling infection of a new host (Molofsky and Swanson, 2004;

79 Oliva *et al.,* 2018). In protozoa such as *Acanthamoeba castellanii*, TP cells were observed to be
80 pleomorphic and eventually matured into highly infectious cyst-like forms with thickened cell
81 walls, multiple membrane laminations and poly-β-hydroxybutyrate (PHB) granules (Faulkner *et*
82 *al.,* 2002; Garduño *et al.,* 2002; Abdelhady and Garduño, 2013; Robertson *et al*., 2014).
83 Development of cyst-like forms has not been observed in human macrophages, likely explaining
84 the near-complete lack of human-to-human transmission (Abdelhady and Garduño, 2013).
85 The biphasic switch between RP and TP is controlled by a stringent response-based
86 regulatory network activated by accumulation of alarmone guanosine tetraphosphate (ppGpp),
87 which is synthesized by RelA and SpoT in response to nutritional deprivation. Synthase RelA
88 senses low amino acid concentrations (Zusman *et al.,* 2002), whereas bifunctional synthase and
89 hydrolase SpoT senses fatty acid flux via acyl carrier proteins (ACP) (Edwards *et al.,* 2009;
90 Dalebroux *et al.,* 2010b). Accumulated ppGpp is associated with activation of the LetA/LetS two
91 component system (TCS), which in turn induces transcription of non-coding RNAs (ncRNAs)
92 RsmY and RsmZ (Hammer *et al*., 2002; Rasis and Segal, 2009; Sahr *et al.,* 2009; Nevo *et al.,*
93 2014). These ncRNAs target and sequester the RNA-binding protein CsrA, thus modulating
94 CsrA-mediated post-transcriptional regulation of transcripts associated with the transition to TP.
95 Such transcripts include those encoding Dot/Icm effectors and those linked to cellular
96 metabolism (Häuslein *et al.,* 2017*;* Sahr *et al*., 2017). Other TCS also play a pivotal role in
97 bacterial differentiation and are often required for virulence in host cells, such as CpxR/A
98 (Feldheim *et al.,* 2016; Tanner *et al.,* 2016); PmrA/B (Zusman *et al.,* 2007; Al-Khodor *et al.,*
99 2009) and quorum sensing via LqsS/T/R (Tiaden *et al.,* 2007; Tiaden *et al.,* 2008; Schell *et al.,*
100 2014; Personnic *et al.,* 2018). In addition, a subset of transcriptional regulators plays an
101 important role in TP induction. IHF assists LetA in the upregulation of RsmY and RsmZ, and is

102 required for full cyst-like form differentiation and virulence in *A. castellanii* (Morash *et al*.,
103 2009; Pitre *et al*., 2013). OxyR regulates transcription of the operon encoding the CpxR/A TCS,
104 linking it to virulence in *A. castellanii* (Tanner *et al.,* 2017). Recently, the autorepressor PsrA
105 was found to be required for optimal intracellular growth and cyst-like form biogenesis in *A.*
106 *castellanii* (Graham *et al*., 2021). While the genetic targets of PsrA have not yet been identified,
107 a potential linkage between PsrA and the core stringent response network has been described
108 with focus on fatty acid flux and an associated ACP (Graham *et al.,* 2021).
109 Accumulated ppGpp also directly affects transcriptomic changes associated with the
110 transition from RP to TP. For example, expression of stationary phase sigma factor RpoS is
111 increased (Dalebroux *et al*., 2010b), which is required for the expression of TP traits and
112 intracellular growth in protozoa such as *A. castellanii* (Hales and Shuman, 1999; Bachman and
113 Swanson, 2001; Zusman *et al.,* 2002; Abu Zant *et al.,* 2006; Hovel-Miner *et al.,* 2009). While the
114 precise mechanism has not yet been ascertained in *L. pneumophila*, ppGpp influences expression
115 most likely by binding directly to RNA polymerase (RNAP), as has been described in *E. coli*
116 where ppGpp binds with equal affinity either to a site encompassed by the ω and β' subunits, or
117 at the interface between RNAP and secondary channel co-factor DksA. DksA features a pair of
118 conserved aspartate residues to enable ppGpp binding (Perederina *et al.,* 2004; Ross *et al*., 2013;
119 Ross *et al*., 2016; Myers *et al*., 2020). The latter event results in a conformational change in both
120 ppGpp and DksA affecting the stability of the open complex generated by the RNAP
121 holoenzyme thereby altering the efficiency of transcription initiation (Chatterji *et al*., 1998;
122 Lemke *et al.*, 2011; Gummesson *et al.,* 2013; Ross *et al*., 2016; Molodtsov *et al.*, 2018). DksA
123 can act independently of ppGpp, compensate for its absence if overexpressed, or even act
124 antagonistically to ppGpp at different promoters (Magnussun *et al.,* 2007; Aberg *et al.,* 2008;

125 Potrykus and Cashel, 2008; Aberg *et al*., 2009). DksA exists in a dynamic equilibrium with
126 structural homologs GreA and GreB in *E. coli*, which compete with DksA for secondary channel
127 binding; if either GreA or GreB binds then DksA-independent ppGpp binding to RNAP still
128 occurs to influence expression (Vinella *et al.,* 2012).

129 *L. pneumophila* encodes both GreA and DksA orthologs, although *L. pneumophila* has
130 not been targeted for study. Like its *E. coli* ortholog, DksA acts independently of, or in
131 coordination with, ppGpp to regulate genes encoding TP traits (Dalebroux *et al.,* 2010b).
132 Previously, DksA was shown to be required in a ppGpp-dependent manner for TP
133 morphogenesis including TP-specific flagellar biosynthesis. Likewise, DksA and ppGpp are both
134 required for optimal intracellular growth in *A. castellanii*. Conversely, DksA, but not ppGpp, is
135 dispensable for intracellular growth in murine macrophages, indicating that ppGpp may act
136 independently of DksA in *L. pneumophila* (Dalebroux *et al.,* 2010b). Thus, the contributions of
137 ppGpp and DksA to the stringent response, are well characterized among the proteobacteria
138 though the mechanisms and targets may vary between them (Gourse *et al*., 2018).

139 In this study, we describe a functional relationship between DksA and PsrA in regulation
140 of virulence in protozoa, discovered fortuitously via a spontaneous secondary mutation within
141 *dksA* in a Δ*psrA* strain background. The *dksA1* mutation was an in-frame deletion of a 24-base
142 pair region that when expressed, produced a truncated but partially functional protein driving a
143 unique phenotype. Through a combination of investigative approaches, we show that PsrA and
144 DksA have distinct and overlapping biological roles in the regulation of TP. Incomplete
145 suppression of phenotypes suggests that PsrA acts in a more targeted manner than DksA, and
146 when interpreted alongside the unusual characteristics of the *dksA1* mutant, infers a high level of

147 regulatory complexity. Taken together, our findings illustrate a complex regulatory interaction
148 between these two proteins, that together act to drive transmissive phase in *L. pneumophila.*
149
150
151
152
153
154
155
156
157
158
159
160
161
162
163
164
165
166
167
168
169

170 **Results**

171 **Spontaneous *dksA1* mutation in Δ*psrA* strain** In a previous study, we deleted *psrA* from the
172 parental *L. pneumophila* Lp02 strain (Graham et al., 2021). Throughout this process, we noted a
173 propensity for some of the isogenic Δ*psrA* strains to acquire secondary mutations in *letS* or *dksA*
174 as discovered through routine whole genome sequencing. One particular Δ*psrA* strain was found
175 to contain an in-frame 24 bp deletion located partway through the *dksA* coding sequence, that
176 resulted in the loss of eight amino acid residues after the 57th residue in the DksA polypeptide.
177 The 57th codon was additionally altered from encoding leucine to phenylalanine. This allele was
178 denoted as the *dksA1* mutation that is characterized in this study (Figure S1A, B).

179 As the truncation appeared in the coiled-coil (CC) domain of DksA, we investigated how
180 the truncation could affect the fold of DksA1 using AlphaFold2 (Jumper *et al*., 2021; Skolnick *et*
181 *al*., 2021). Both DksA and DksA1 were submitted to the colabfold2 server (AlphaFold2) with
182 default settings and were modelled with a moderate-to-high degree of confidence (Figure S1C,
183 D). The CC domain of DksA was well built as was the majority of the globular-head (GH)
184 domain. Conversely, the eight-amino acid truncation in DksA1 resulted in a partial disruption of
185 the tip of the CC domain with AlphaFold predicting a 'disordered' loop with moderate
186 confidence (Figure S1D). The extent of the potential structural changes in the mis-formed tip of
187 the CC domain in DksA1 can be observed when overlayed with a previously solved structure of
188 a DksA:RNAP complex from *E. coli* (PDB ID: 5VSW) (Molodtsov *et al*., 2018). As shown in
189 Figure 1A, all DksA variants align well, except for the altered CC-loop regions near helix α3 and
190 the C-terminal region helix α5 not present in the DksA *E. coli* crystal structure. Importantly, the
191 truncation did not delete key function residues shown to be needed for interaction of DksA with
192 the RNAP allosteric (K104, L101, K100, R97) or with the RNAP active site (D80, D77) (Parshin
193 *et al*., 2015; Molodtsov *et al*., 2018) (Figure 1B). Furthermore, all DksA variant structures can be

194 modeled into RNAP (Figure S2) slotting into the allosteric site (Figure 1C) and RNAP active site
195 (Figure 1D) without significant variation from the experimental DksA structure. However, while
196 the AlphaFold predictions for Lp02 DksA and DksA1 had a properly modeled ppGpp binding
197 site (Figure 1E), the twin-aspartate loop of the CC domain was significantly altered in DksA1
198 through the shift of D69 (D71 in DksA) by ~8.9Å (Figure 1F). These models therefore suggest
199 that while the functional residues are conserved from the truncation, DksA1 should be incapable
200 of coordinating the Mg^{2+} in the active site of RNAP. Conversely, the structural predictions show
201 that DksA1 is likely still able to bind RNAP. Specifically, DksA1 is predicted to still contact the
202 secondary binding site of ppGpp functionally as an allosteric inhibitor of RNAP through ppGpp
203 mediated recruitment.

204

205 **PsrA partially rescues the growth defect of the *dksA1*, but not Δ*dksA*, strain in *A. castellanii***
206 Given the previously described regulatory roles of DksA and PsrA (Dalebroux *et al.,* 2010b;
207 Graham *et al.,* 2021), the discovery of the Δ*psrA dksA1* mutant strain, and in turn the
208 backtracked ancestral *dksA1* mutant strain, presented a fortuitous opportunity to investigate
209 potential genetic links between the two regulatory factors in the established protozoan infection
210 model *A. castellanii*. To test our hypothesis, we electroporated the *in trans psrA* expression
211 vector (originally referred to as pComp in Graham *et al*., [2021] henceforth renamed to pComp-
212 *psrA* in this study), or empty control vector pThy, into the mutant strains. Intracellular growth
213 kinetics were conducted on *dksA1* pThy, Δ*psrA* pThy, *dksA1* Δ*psrA* pThy, and *dksA1* pComp-
214 *psrA* strains, along with virulent Lp02 pThy and avirulent Δ*dotA* pThy strains as controls, at
215 25ºC over 168 h as previously described (Tanner *et al.,* 2016; Graham *et al*., 2021) (Figure 2A).
216 The profiles of Lp02 pThy and Δ*dotA* pThy strains were as expected demonstrating ~ three-$\log_{10}$

217 increases in titre, and titres staying near initial inoculum density, respectively. The *dksA1* pThy
218 and Δ*psrA dksA1* pThy strains showed no significant increase in titres indicating that the
219 chromosomal single copy *dksA1* mutation was defective for virulence. Surprisingly, PsrA
220 overexpression in the *dksA1* background resulted in a two-$\log_{10}$ recovery of growth ($p = 0.0006$)
221 to a titre within one-$\log_{10}$ of the Lp02 pThy strain. This suggested that elevated levels of PsrA
222 were able to partially, but not fully, rescue the avirulent phenotype demonstrated by the *dksA1*
223 strain. While a genomic copy of *psrA* is present in the *dksA1* strain, it was shown previously that
224 *in trans* overexpression of PsrA from pComp-*psrA* resulted in an elevated quantity of cellular
225 protein that not only rescued the reduced growth phenotype associated with gene deletion of
226 *psrA*, but also enhanced replicative growth of Lp02 in *A. castellanii* (Graham *et al.*, 2021).
227 Nevertheless, the surprising ability of PsrA to partially complement the growth defect of *dksA1*
228 led us to expand our investigations to define the relationship between the two regulatory factors.
229 A previous study elsewhere reported that an insertional *dksA* mutant showed a modest
230 intracellular growth defect in *A. castellanii* at 37°C with slow growth initially, but eventually
231 achieving similar titres to parental Lp02 by the end of the 96 h experiment (Dalebroux *et al,*
232 2010b). This reported phenotype differs in comparison to the significantly reduced intracellular
233 growth observed with the *dksA1* strain in this study. This difference supported our hypothesis
234 that the truncated DksA1 protein bore altered function and distinct phenotype versus the null
235 mutant. To further test this hypothesis, and to determine if the compensatory effect of *psrA*
236 observed with the *dksA1* mutant strain extended to a null deletion mutant strain, we generated an
237 unmarked, in-frame Δ*dksA* isogenic strain, as well as the double Δ*dksA* Δ*psrA* mutant strain.
238 Complementation of DksA was achieved by cloning *dksA* and its native promoter into pJB908
239 creating pComp-*dksA* for electroporation into the Δ*dksA* strain. Plasmid pComp-*psrA* was also

240 electroporated into the Δ*dksA* strain to test if the rescue of the growth defect in *dksA1* by PsrA
241 overexpression was reproducible. Empty control vector pThy were electroporated into both
242 Δ*dksA* and Δ*dksA* Δ*psrA* strains. The intracellular growth kinetics of the generated strains were
243 assessed in *A. castellanii* under the same conditions as before along with Lp02 pThyA and Δ*dotA*
244 pThyA as control strains (Figure 2B). Interestingly, the single Δ*dksA* pThy and double Δ*dksA*
245 Δ*psrA* pThy mutant strains were both fully avirulent, starting at a slightly lower titre than the
246 Δ*dotA* pThy strain, then declining to, or below, the detection limit of the assay (~10 CFU/mL).
247 The severe growth defect of the Δ*dksA* pThy strain was fully rescued by *in trans* expression of
248 *dksA*, but not *psrA*; a notable divergence from the rescued phenotype demonstrated by the *dksA1*
249 pComp-*psrA* strain. Taken together, the lack of DksA results in a complete avirulent phenotype
250 in these conditions which cannot be rescued by PsrA, whereas the partially functional DskA1 has
251 a less severe impact on intracellular growth that can be partially rescued by PsrA.
252
253 **DksA1 rescues the growth defect of the Δ*dksA* strain, and vice versa, in *A. castellanii*** Given
254 that DksA can rescue the severe growth defect of the Δ*dksA* strain in *A. castellanii* (Figure. 2B),
255 we next asked if the partially functional DksA1 could likewise do so despite the truncation in the
256 coiled-coil structure (Figure 1). To this end, the *dksA1* gene and its native promoter was cloned
257 from the *dksA1* genome into pJB908, creating pComp-*dksA1,* which was electroporated into
258 Δ*dksA* to generate the Δ*dksA* pComp-*dksA1* strain for assessment in *A. castellanii*, along with
259 Δ*dksA* pThy, and Lp02 pThy and Δ*dotA* pThy as control strains (Figure 2C). The severely
260 reduced growth phenotype of the Δ*dksA* pThy strain was robustly rescued as by *in trans*
261 complementation with DksA1 as shown by the growth profile of the Δ*dksA* pComp-*dksA1* strain
262 (p = 0.0002) matching that of the Lp02 pThy strain. It should be noted that this growth

263 phenotype contrasted with the minimal growth profile of the Δ*dksA1* pThy strain (Figure 2A),
264 suggesting that restoration of the virulent phenotype of the Δ*dksA* strain was due to plasmid-copy
265 number driven overproduction of DksA1 protein (pComp-*dksA1*), sufficient to offset the
266 structural and functional inefficiency caused by the intragenic 24 bp deletion. Not unexpectantly,
267 *in trans* complementation of DksA successfully rescued the avirulent phenotype of the *dksA1*
268 pThy strain to match the growth profile of Lp02 pThy as the plasmid-copy number driven
269 production of DksA outnumbered that of DksA1 (Figure 2D). In the reverse scenario, the growth
270 profile of Lp02 pComp-*dksA1* still matched that of Lp02 pThy suggesting that despite the
271 plasmid-copy number driven production of DksA1, the chromosomal-copy production levels of
272 DksA and PsrA in parallel were each sufficient to disguise any effects caused by the
273 dysfunctional DksA1 (Figure 2A, Figure 2D).
274
275 **DksA restores the growth defect of the Δ*psrA* strain in *A. castellanii*** To further define the
276 relationship between DksA and PsrA, we next asked if DksA could reciprocally compensate for
277 lack of PsrA or generally, affect intracellular growth in the presence of PsrA. To this end,
278 pComp-*dksA* was electroporated into parental Lp02 and Δ*psrA* strains and then assessed for
279 growth in *A. castellanii* along with the Lp02 pThy and Δ*dotA* pThy strains as controls, and the
280 Δ*psrA* pThy strain for comparative purposes (Figure 2E). As previously reported, the Δ*psrA*
281 pThy strain consistently maintained 1 $\log_{10}$ lower than that of Lp02 pThy (p = 0.029) (Graham *et*
282 *al*., 2021). The mean growth profile of the overexpression Lp02 pComp-*dksA* strain showed a
283 subtle increase of ~½ $\log_{10}$ over that of Lp02 pThy (p = 0.007); this enhancement could also be
284 seen in the Δ*dksA* pComp-*dksA* complemented strain (Figure 2D; p = 0.0247). Likewise, we
285 found that *in trans* expression of DksA in the Δ*psrA* pComp-*dksA* strain rescued the growth

286 defect of Δ*psrA* strain, increasing growth by ~1 $\log_{10}$ to match that of Lp02 pThy strain ($p <$
287 0.001 versus Δ*psrA* pThy, not significant versus Lp02 pThy). Although this experiment did not
288 generate large phenotypic differences, we found the tendency towards subtle phenotypes upon *in*
289 *trans* expression of DksA to be noteworthy relative to the very strong phenotypes noted in the
290 *dksA* mutant strains.
291
292 **DksA is not required for intracellular growth in human U937-derived macrophages**
293 Some *L. pneumophila* genes exhibit host specific requirements; being required only for growth in
294 one host type, but not in another. Previous work with *L. pneumophila* showed that the human
295 U937-derived macrophage host model is more permissive to regulatory mutants than *A.*
296 *castellanii*, as exemplified by transcriptional regulator Δ*psrA* or Δ*cpxRA* TCS mutants (Tanner *et*
297 *al.,* 2016; Graham *et al.,* 2021). DksA was previously shown to be dispensable for growth in
298 primary murine bone marrow macrophages (Dalebroux *et al.,* 2010b); however, since the
299 phenotype we observed for a Δ*dksA* strain in *A. castellanii* was different from that reported by
300 Dalebroux *et al*. (2010b), we decided to verify the phenotype in mammalian macrophages.
301 Intracellular growth kinetics were assessed for the same set of strains used in the *A. castellanii*
302 infection assays (Figure 2) in the human U937-derived macrophage infection model. As
303 expected, positive control Lp02 pThy grew well, increasing approximately 100-fold by the 72 h
304 timepoint (Figure 3A), and negative control Δ*dotA* pThy maintained a steady titre with no
305 growth. In comparison to that of Lp02 pThy, Δ*dksA* pThy and *ΔdksA ΔpsrA* pThy strains showed
306 similarly robust, but offset (delayed) growth profiles. Additionally, despite normalization of the
307 inoculum by OD_{600}, these two strains showed initial measured titres lower than that of Lp02
308 pThy (Figure 3A). Only *ΔdksA ΔpsrA* pThy showed a significant deviation from the parental

309 strain (p = 0.049). The Δ*dksA* pComp-*psrA* showed a similar profile to the parental strain (Figure
310 3A), and did not show the reduced starting titre, but the difference to Δ*dksA* pThy was not
311 significant. No significant change in phenotype was observed with the remaining set of strains
312 featuring *in trans* DksA expression, either by complementation (Δ*dksA* pComp-*dksA*),
313 overexpression, (Lp02 pComp-*dksA*) or in Δ*psrA* pComp-*dksA* (Figure 3B). The growth profiles
314 of the *dksA1* pThy, *dks1* Δ*psrA* pThy, or *dksA1* pComp-*psrA* were indistinguishable from Lp02
315 pThy (Figure 3C) and lacked even variability in the initial uptake. Thus, these results verify that
316 DksA is not required for, nor does it enhance, intracellular growth in mammalian macrophages.
317
318 ***In vitro* growth is impacted by DksA, PsrA and DksA1** The differences observed with the
319 intracellular growth kinetics of isogenic mutant and complemented strains in *A. castellanii* may
320 be in part due to defects in the growth rates of the cells, rather than solely virulence defects *in*
321 *vivo*. To distinguish this possibility and more generally characterize the *in vitro* growth
322 characteristics of the strains, we tested the *in vitro* growth rates of the strains in BYE broth at
323 37ºC over a 24-hour time period (Figure 4). The growth profiles of the first set of strains (*dksA1*
324 pThy, *dksA1* Δ*psrA* pThy, *dksA1* pComp-*psrA*, *dksA1* pComp-*dksA*) (Figure 4A) were similar to
325 each other, and to that of Lp02 pThy. The growth profiles of the second set of strains (Δ*psrA*
326 pThy*, psrA* pComp-*dksA*, Lp02 pComp-*dksA*, Lp02 pComp-*dksA1*) were slightly varied.
327 Consistent with our previous study, the growth profile of Δ*psrA* pThy was significantly reduced
328 in comparison to that of Lp02 pThy (p = 0.036; Figure 3B) (Graham *et al*., 2021). For the DksA
329 overexpression Lp02 pComp-*dksA* and DksA-complemented Δ*psrA* pComp-*dksA* strains,
330 plasmid-driven overproduction of DksA seemed to slightly reduce the growth profiles in
331 comparison to the growth profiles of Lp02 pThy and Δ*psrA* pThy, respectively (both $p < 0.001$;

332 Figure 4B). Conversely, overexpression of DksA1 had no effect as the growth profiles of Lp02
333 pComp-*dksA1* and Lp02 pThy were similar.

334 Interestingly, the *in vitro* growth kinetics of Δ*dksA*-based strains featured a phenotype of
335 growth variability across replicates as manifested by the large error bars for hourly data points
336 (Figures 4C, 4D). This growth variability made the determination of statistical significance
337 difficult when comparing growth profiles of mutant and/or complemented strains to that of Lp02
338 pThy. This is exemplified by the growth profiles of Δ*dksA* pThy and Δ*dksA* Δ*psrA* pThy strains
339 of which both appeared to be elevated in comparison to that of Lp02 pThy (Figure 4C), but the
340 difference was not statistically significant. This variability is also seen with the Δ*dksA* pComp-
341 *psrA* and Δ*dksA* pComp-*dksA1* growth profiles, with the former not rescued and the latter
342 generating a growth profile significantly reduced in comparison to that of Lp02 pThy ($p <$
343 0.0001; Figure 4C). Notably, the growth variability disappeared from the Δ*dksA* pComp-*dksA*
344 growth profile suggesting this was a complementable phenomenon. The growth additionally was
345 slightly reduced in comparison to that of Lp02 pThy (p=0.017), likely due to plasmid-copy
346 number driven overproduction of DksA. Conversely, the DksA1 overexpression Lp02 pComp-
347 *dksA1* strain produced a growth profile matching that of the parental Lp02 pThy strain (Figure
348 4B) with minimal growth variability across replicates. This suggests that elevated levels of
349 DksA1 imparts a negative effect on replicative growth in absence of the parental *dksA* allele.

350 The *in vitro* growth profile assays were repeated at 25°C, albeit over a 48-hour time
351 period to account for the slower growth rate, to mimic the incubation temperature of the *A.*
352 *castellanii* assays. The resultant growth profiles were mostly similar to those attained at 37°C,
353 with growth variability of strains lacking *dksA* exacerbated at 25°C as indicated by data points
354 with widened error bars (Figure 5). One notable difference was that the growth profile of Δ*dksA*

355 pComp-*dksA1* strain matched that of Lp02 pThy at 25°C (Figure 5C), versus the reduction at
356 37°C (Figure 4C), suggesting that the slower growth rate and/or lower temperature
357 accommodated the dysfunctional nature of DskA1.

358 These findings together suggest that while strains lacking *dksA* featured more variability
359 in growth profiles, more so at 25°C then at 37°C, the *in vitro* growth assays (Figures 4 and 5)
360 illustrates that the observed *in vivo* growth defects are specific to *A. castellanii* (Figure 2), and
361 not due to poor growth of the bacterial cells themselves.

362

363 **DksA, and possibly PsrA, mediates cell morphology** Throughout this study, it was noted that
364 the colony morphologies of Δ*dksA* and *dksA1* strains grown on BCYE agar plates differed
365 significantly from that of parental Lp02. In comparison to the opaque beige-white glossy
366 colonies with varied margins featured by Lp02, Δ*dksA* colonies were textured glossy white with
367 defined margins, and *dksA1* colonies were smooth glossy white with defined margins. The
368 phenotypes were particularly evident when 10 µL of OD_{600} = 0.15 bacterial suspensions in broth
369 were spotted onto BCYE plates as were done in serial dilution assays in this study (Figure 6). For
370 both Δ*dksA* and *dksA1* strains, the phenotype was fully rescued by *in trans* complementation of
371 DksA whereas *in trans* DksA1 complementation partially rescued Δ*dksA*. The colony
372 morphology of the Δ*dksA* Δ*psrA* was similar to that of the Δ*dksA* strain, but not to the Δ*psrA*
373 strain which was similar to that of the parental strain indicating the sole influence of DksA.
374 Finally, *in trans* PsrA complementation did not appear to alter colony morphology in all strain
375 backgrounds assessed (Lp02, Δ*dksA*, *dksA1,* Δ*psrA*), confirming that PsrA does not influence
376 this phenotype.

377 We previously reported that PsrA promoted cell elongation when overexpressed *in trans*
378 (Graham *et al.,* 2021). Conversely, it was reported elsewhere that lack of DksA influenced cell
379 elongation (Dalebroux *et al*., 2010b). To assess whether a genetic relationship between PsrA and
380 DksA was evident in cell structure morphology, and to further explore whether *dksA1* generated
381 a phenotype distinct from Δ*dksA*, bacteria were inoculated into BYE broth from OD_{600} = 0.02
382 and grown overnight to OD_{600} = ~0.5, (exponential growth phase; EP), or another 24 h beyond
383 (stationary phase; SP) respectively, for microscopic analyses (Figure 7). Cell lengths were
384 quantified by measuring cells with the length tool in ImageJ and plotted separately for analysis
385 (Figures 8A and 8B). As a control, Lp02 pThy bacteria formed typical rods (mean length 3.6
386 µm) in EP, that elongated into SP (mean length 5.8 µm). The Δ*dksA* pThy bacteria were notably
387 elongated in EP (mean length 6.2 µm) and, in SP, became extremely elongated into filamentous
388 forms often of sufficient length to often exceed the field of view, averaging 13.2 µm among
389 measurable cells (with the entire cell visible in one field of view). Likewise, the Δ*dksA* Δ*psrA*
390 pThy bacteria were also elongated in EP, and strongly filamentous in SP (mean lengths 5.4 µm
391 and 17.1 µm, respectively). Conversely, Δ*psrA* pThy bacteria were morphologically
392 indistinguishable to Lp02 pThy, as previously observed (Graham *et al*, 2021). The Δ*dksA*
393 pComp-*dksA* bacterial forms resembled those of Lp02 pThy indicating that filamentation was
394 rescued by DksA complementation: they were slightly but significantly shortened relative to
395 Lp02 (2.9 µm and 4.7 µm in EP and SP phases, respectively). Expression of DksA *in trans* in
396 Δ*psrA* pComp-*dksA* and Lp02 pComp-*dksA* strains also resulted in slightly, but significantly
397 shorter cell lengths in comparison to those of Lp02 pThy and comparable to Δ*dksA* pComp-*dksA*
398 in both growth phases, suggesting the shortening mediated by DksA is independent of PsrA.

399 PsrA complementation in Δ*dksA* pComp-*psrA* did not strongly affect the bacterial cell lengths
400 and elongation was still present (7.5 µm and 14.2 µm in EP and SP, respectively).
401 Conversely, the *dksA1* pThy, *dksA1 ΔpsrA* pThy, and *dksA1* pComp-*psrA* were slightly
402 elongated relatively to parental Lp02 pThy in both EP (5.0 µm, 5.1 µm and 4.3 µm, respectively)
403 and SP (7.5 µm, 7.7 µm, and 7.8 µm, respectively) but were not filamentous, and did not vary
404 significantly from each other again supporting the hypothesis that the *dksA1* allele maintained
405 partial function. Interestingly, the Δ*dksA* pComp-*dksA1* strain did not show complementation of
406 the elongation to resemble *dksA1* levels as might be expected (5.6 µm in EP, 12.3 µm in SP). To
407 rule out the simple possibility of the two gene products conflicting in some way, we tested *dksA1*
408 pComp-*dksA*, that reversed the alleles expressed on plasmid and the chromosome, and this strain
409 appeared somewhat shortened relative to parental Lp02 pThy in SP only (4.2 µm) resembling the
410 other *in trans dksA* overexpression strains, suggesting that relative protein concentrations may
411 drive the phenotype. Together, this indicates that the previously reported role of *psrA* is
412 overshadowed by the more potent role of DksA, and that the DksA1 protein shows an
413 intermediate phenotype illustrating that DksA1 is a partially functional protein in these strains.
414
415 **DksA or DksA1 are necessary for extended culturability in depleted media** Previously, the
416 insertional Δ*dksA* strain was also noted to feature reduced recovery of culturable bacteria after
417 extended incubation in depleted media, which the authors referred to as "survival" (Dalebroux *et*
418 *al.,* 2010b), although the assay attempted to recover culturable rather than viable bacteria. Over
419 the course of this study, we noticed that the Δ*dksA* mutants could not be consistently sub-
420 cultured (likely contributing to the variability of these strains seen in Figure 3), or often failed to
421 grow entirely if taken from plates grown more than three days, ordinarily easily possible with

422 parental strains. In view of this, we asked if this was a consequence of previously observed
423 culturability phenotype occurring in the unmarked Δ*dksA* mutant, and potentially the *dksA1*
424 strains, and whether PsrA may also contribute. As this phenotype had not been assessed in the
425 prior PsrA study (Graham *et al.*, 2021), we decided to include Δ*psrA* pThy, Δ*psrA* pComp-*psrA*
426 and Lp02 pComp-*psrA* (*psrA* overexpression) strains from Graham *et al.* (2021). The bacteria
427 from each strain were suspended in BYE at $OD_{600} = 0.15$, and grown at 37°C for 96 hours with
428 shaking, with samples taken for optical density values and CFU/mL titres at 24 h intervals.
429 Over the time course, optical density values peaked comparably for all strains at 24 h,
430 and held steadily to the 96 h timepoint (Figure 9). Enumeration of titres for Lp02 pThy and
431 Δ*psrA* pThy were comparable to one another, but the titres for Δ*dksA* pThy and Δ*psrA* Δ*dksA*
432 pThy were significantly reduced by 72 h, and more so by the 96 h for Δ*dksA* pThy, noting that
433 titre enumeration was not possible for Δ*psrA* Δ*dksA* pThy at 96 h as no colonies were recovered
434 in any replicate for this strain at that timepoint (detection limit ~10^2 CFU/mL; Figure 9A). The
435 reduced culturability phenotype was rescued by *in trans* complementation of DksA or DksA1,
436 but not PsrA (Figures 9B, 9C). The extended culturability of *dksA1* pThy strain was unaffected
437 in comparison to parental Lp02 pThy, thereby not requiring nor significantly benefiting from
438 plasmid-borne *in trans* complementation of DksA (Figure 9D). The unaltered phenotype of
439 *dskA1* Δ*psrA* pThy and Δ*psrA* pComp-*dksA* strains further supports the observation that PsrA
440 does not contribute to, nor does overexpression of DksA (i.e. Lp02 *pComp-dksA*) significantly
441 improve, extended culturability (Figures 9E, 9F). Thus, in summary, PsrA plays no role in
442 extended culturability, while DksA is essential for the culturability of Lp02 in depleted media as
443 reported elsewhere previously (Dalebroux *et al.,* 2010b). Notably, the hypomorph *dskA1* allele
444 has retained this essential function of promoting extended culturability.

445 **Pigmentation requires fully functional DksA, but not PsrA** *L. pneumophila* pigment is a
446 brown, melanin-like secreted protein that is released into the supernatant during the transition to
447 stationary phase under the control of the stringent response through RelA (Zusman *et al*., 2002;
448 Dalebroux *et al.*, 2010b). Further, we observed hyperpigmentation of a subset of parental,
449 isogenic (Δ*psrA*, Δ*dksA*) and *dksA1* strains overproducing *dksA in trans* (Figure 10A). To
450 ascertain whether DksA1 and/or PsrA could contribute to this hyperpigmentation, we quantified
451 the pigmentation for each strain by measuring absorbance of the bacterial culture supernatant at
452 550 nm as done elsewhere (Wiater *et al.*, 1994; Dalebroux *et al.,* 2010b) (Figure 10B).
453 The parental Lp02 pThy strain developed moderate pigmentation (Abs_{550}/OD_{600} = ~0.20)
454 that was similarly achieved by Δ*psrA* pThy, Δ*psrA* pComp-*psrA*, and Lp02 pComp-*psrA* strains
455 suggesting that PsrA does not influence pigmentation (Figure 10B). This supposition is further
456 borne out by the significantly reduced pigmentation (Abs_{550}/OD_{600} = 0.10 - 0.12) featured by
457 both of the Δ*dksA* Δ*psrA* pThy and Δ*dksA* pThy strains, which the latter is rescued to
458 significantly increased levels (i.e. hyperpigmentation) (Abs_{550}/OD_{600} = 0.36 - 0.38) over that of
459 Lp02 pThy likely due to plasmid-copy number driven overproduction of DksA (Figure 10B).
460 Indeed, the pigmentation phenotype was rescued by *in trans* DksA complementation in the
461 Δ*psrA* strain background, but not by *in trans* PsrA complementation in the Δ*dksA* strain
462 background, clearly indicating that only DksA positively influences pigmentation (Figure 10B).
463 Pigmentation was also significantly reduced (Abs_{550}/OD_{600} = 0.05 - 0.09) in the *dksA1* pThy and
464 *dksA1* Δ*psrA* strain backgrounds, and the phenotype is not rescued by *in trans* PsrA
465 complementation verifying the lack of involvement in pigmentation by PsrA (Figure 10B).
466 Surprisingly, the hypomorph DksA1 could not rescue pigmentation in the Δ*dksA* strain, but
467 pigmentation of *dksA1* strain could be induced by *in trans* DksA complementation. The *dksA1*

468 pComp-*dksA* strain showed delayed onset of hyperpigmentation such that only one of three
469 replicates had fully pigmented by 30 h; all replicates of this strain pigmented by 48 h (Figure
470 10A), but at 30 h the difference was not statistically significant. These findings indicate that the
471 ability of DksA1 to interact with RNAP is impaired as suggested by structural modelling
472 (Figures 1, 10B). Taken together, these findings indicate that DksA is sufficient to drive
473 pigmentation independent of PsrA, although, curiously the *dksA1* strain was unpigmented like
474 the Δ*dksA* strain, which can be interpreted as the truncated region impacting this phenotype for
475 more than, for example, extended culturability where no significant impact was observed.
476
477 **Growth in long chain fatty acids is mediated by PsrA and DksA** The activation of the
478 biphasic switch is mediated in part by the response to fatty acid flux (Edwards *et al.,* 2009;
479 Dalebroux *et al.,* 2010b). It was shown elsewhere that *in vitro* supplementation of short chain
480 fatty acids (SCFAs), such as propionic acid, will trigger the expression of transmissive phase
481 traits (Edwards *et al.,* 2009). Further, the process of differentiation in response to excess SCFAs
482 is mediated by DksA (Dalebroux *et al.,* 2010b). Likewise, PsrA is associated with differentiation
483 and although the precise role remains to be elucidated, the *Pseudomonas* PsrA ortholog is a
484 sensor of long chain fatty acids (LCFAs), presence of which alleviates PsrA-mediated repression
485 of the *fadBA5* β-oxidation operon (Kang *et al*., 2008). In this view, Δ*psrA* and complemented
486 strains were grown in BYE broth supplemented with the LCFA, palmitic acid, to determine if
487 bacterial growth was impacted by lack of PsrA. In comparison to normalized Lp02, 2-fold
488 inhibition of growth of the Δ*psrA* pThy strain was observed which was rescued by *in trans* PsrA
489 expression strongly suggesting the involvement of PsrA in responding to LCFAs (Figure 11A).
490 Because chromosomal DksA expression is present in the Δ*psrA* pThy strain, we next asked if

491 DksA had a contributing factor in responding to palmitic acid which could be amplified through
492 *in trans* DksA expression in the Δ*psrA* strain background. While it appears that growth of the
493 Δ*psrA* pComp-*dksA* strain improved, it was not statistically significant (Figure 11A). Likewise,
494 *in trans* DksA expression in the parental strain background did not significantly improve
495 bacterial growth over that of the parental strain alone (Figure 11A). To further investigate the
496 role of DksA, Δ*dksA*-based strains were assessed in palmitic acid-supplemented BYE media. As
497 expected, the double Δ*dksA* Δ*psrA* pThy strain had 2-fold growth inhibition with less variability
498 amongst the data points than in comparison to the Δ*psrA* pThy strain by itself (Figure 11A, 11B).
499 Growth inhibition of the Δ*dksA* pThy strains was not considered statistically different from the
500 normalized growth of Lp02 (Figure 11B). Conversely, *in trans* DksA expression significantly
501 improved bacterial growth over that of normalized Lp02 (Figure 11B). Surprisingly, *in trans*
502 PsrA expression in the Δ*dksA* strain background could not fully rescue the growth inhibition
503 phenotype. Taken together, these results suggest that while PsrA is largely responsible for the
504 response to LCFAs, DksA also contributes additively to this response lending support to the
505 overlapping roles observed for the two regulatory factors for some of the traits in this study.
506
507
508
509
510
511
512
513

514 **Discussion**

515 The biphasic lifecycle of *L. pneumophila* is controlled by the convergence of multiple signals
516 into a sophisticated regulatory network that ultimately acts to induce TP differentiation. The
517 primary signals driving differentiation link to the nutritional status of the environment, mediated
518 largely by induction of the stringent-response and the associated downstream regulatory network
519 in association with RNAP-binding cofactor DksA, alternative sigma factor RpoS, two-
520 component systems and a subset of transcriptional regulators including PsrA (Fonseca and
521 Swanson, 2014; Oliva *et al*., 2018; Graham *et al*., 2024).

522 This study investigated a spontaneous *dksA* mutation, termed *dksA1*, resulting in a
523 truncated DksA1 protein featuring a deletion within its CC domain (Figure 1) (Perederina *et al,*
524 2004; Dalebroux *et al.,* 2010b). The Δ*dksA1* strain showed reduced intracellular growth in *A.*
525 *castellanii* protozoa that was partially, but not fully, rescued by *in trans* expression of *psrA*
526 allowing us to propose *dksA1* and encoded protein product as representing a partially functional
527 allele whose phenotypes allowed us to explore overlapping cellular functions of both regulators,
528 inferring an overlap of gene targets regulated by DksA and PsrA (Figure 2A).

529 The intermediate phenotype observed in bacteria expressing DksA1 relative to DksA can
530 be explained by comparing their AlphaFold2 models to that of *E. coli* DksA bound to RNAP
531 (Figure 1) (Molodtsov *et al*., 2018). These models predict DksA1 to be physically incapable of
532 coordinating magnesium in the active site of RNAP due to the truncated loop in the CC domain
533 (Figure 1D, F). However, DksA1 is still predicted to overall form the core CC and GH domains
534 (Parshin *et al*., 2015; Molodtsov *et al*., 2018). This would hypothetically still allow DksA1 to
535 bind into the allosteric binding pocket of RNAP (Figure 1C, S2) thereby recruiting a secondary
536 ppGpp to RNAP. This would partially explain the variance in phenotype of *dksA1* as an
537 intermediary between the WT and knockout strain. Likewise, these structural predictions also fit

538 into the model of the interplay between GreA and DksA as allosteric inhibitors/activators of
539 RNAP competing for the same allosteric site (Parshin *et al*., 2015; Molodtsov *et al*., 2018).
540 To explore the possibilities that either DksA and PsrA genetically interact with each
541 other, or act in parallel, Δ*dksA* and Δ*dksA* Δ*psrA* strains were subsequently assessed for growth
542 kinetics in *A. castellanii* protozoa (Figure 2). The Δ*dksA* strain developed a more severely
543 avirulent phenotype than the *dksA1* strain, and was rescued by *in trans* complementation of *dksA*
544 and by *dksA1*, but not by *psrA*. Notably, the avirulent phenotype of the Δ*dksA* pThy strain
545 contrasts to previous experiments showing that a Δ*dksA* insertional mutant strain exhibited
546 reduced intracellular growth, but was not avirulent in *A. castellanii* (Dalebroux *et al.,* 2010b).
547 This discrepancy in findings could be due to differing experimental conditions as Dalebroux *et*
548 *al.* (2010b) conducted *A. castellanii* infections at 37°C. Temperature-dependent phenotypes have
549 been seen previously, for example, with Δ*hfq* mutant strains, which only showed an intracellular
550 kinetic defect in *A. castellanii* at 30°C, but not at 37°C (McNealy *et al.,* 2005). We undertook the
551 *A. castellanii* infections at 25°C and showed that the avirulent phenotype of Δ*dksA* was fully
552 complemented by *in trans* DksA expression (Δ*dksA* pComp-*dksA*) indicating that the phenotype
553 was solely due to the genetic deletion of *dksA*. Another possibility for the discrepancy is the
554 possibility of different deletion strategies causing polar effects; Sahr *et al* (2012) annotated *L.*
555 *pneumophila* Paris strain *dksA* in an operon with an uncharacterized alpha/beta hydrolase
556 *lpp2286* encoded downstream and Lp02-derivative strains are likely similar. However, both our
557 study and the previous work by Dalebroux *et al* (2010b) showed the respective mutants were
558 complementable and thus, the discrepancy is unlikely a polar effect, although the previous work
559 did not test this in their intracellular kinetics assay. Additionally, *in trans* expression of DksA1
560 was sufficient to compensate for lack of DksA indicating that the mutant truncation did not

561 impact essential function of DksA. Lastly, expression of DksA enhanced and rescued
562 intracellular growth in Lp02 and Δ*psrA* strains, respectively. Thus, DksA can compensate for
563 lack of PsrA, and PsrA can partially compensate for the reduced activity of DksA1, but cannot
564 compensate for the absence of DksA intracellularly in *A. castellanii*. Taken together, the
565 interplay of DksA and PsrA in regulating their gene targets is not fully reciprocal, indicating that
566 successful intracellular growth in *A. castellanii* is largely driven by DksA with assistance from
567 PsrA.

568 The requirement of DksA for intracellular growth is host specific. DksA was shown
569 elsewhere to be dispensable for growth in primary murine macrophages (Dalebroux *et al*.,
570 2010b) and for human U937-derived human macrophages as shown in this study (Figure 3).
571 Likewise, the Δ*dksA* Δ*psrA* strain was not impeded for intracellular growth in U937-derived
572 macrophages; a finding similar to that previously found with the Δ*psrA* strain (Graham *et al*.,
573 2021). Overexpression of DksA in the Lp02 strain background enhanced intracellular growth in
574 protozoa, but with little overall impact in U937-derived macrophages, a trend also seen with
575 overexpression of PsrA (Graham *et al*., 2021), indicating that elevated levels of either regulatory
576 factor on an individual basis imbued a positive effect on replication in *A. castellanii* that did not
577 equate to a substantial phenotype in U937-derived macrophages.

578 The induction of regulatory mechanisms controlling the transition switch from RP to TP
579 are generally comparably induced *in vivo* (e.g. in protozoa) and *in vitro* (Byrne and Swanson,
580 1998), thus enabling *in vitro* approaches to examine growth kinetics and phenotypes
581 characteristic of TP-associated traits of *L. pneumophila*. To this end, *in vitro* kinetic assays were
582 undertaken to show the interplay between DksA and PsrA were largely growth temperature-
583 independent (Figures 4 and 5). While the Δ*dksA* mutant strain featured erratic but generally

584 enhanced growth, incrementally increased *in trans* expression of DksA in Δ*dksA* and parental
585 strains, respectively, inhibited growth in broth. This phenotype was inverse to that seen of the
586 Δ*dksA* strain harboring chromosomal and *in trans* expression of PsrA which positively impacted
587 growth within protozoa (Figure 2B). Moreover, the Δ*psrA* pComp-*dksA* strain grew slower than
588 either Δ*psrA* or Lp02 pComp-*dksA* strains individually in broth, suggesting the presence of an
589 additive effect (Figures 4D). The slowest growing strain in broth was Δ*dksA* pComp-*dksA1*,
590 indicating that the mutant truncation bore functional consequence towards growth rates, a
591 curious discrepancy when compared with the growth rate of this strain in protozoa, which
592 resembled the parental Lp02 (Figures 2C, 4C). The slow *in vitro* growth phenotype did not apply
593 to the *in vivo* grown Lp02 pComp-*dksA1* strain bearing chromosomally expressed DksA,
594 inferring that DksA1 is not a dominant-negative allele (Figure 2D) and suggesting an underlying
595 complexity to the altered function of the mutant protein. Taken together, the *in vitro* growth
596 kinetic profiles were consistent with the current model of DksA promoting TP-associated traits
597 (Dalebroux *et al.,* 2010b).

598 Other phenotypes such as cellular filamentation, pigmentation, and recovery of culturable
599 bacteria from depleted media, were consistent with previously reported findings (Dalebroux *et*
600 *al.,* 2010b). Lack of DksA resulted in unusual colony morphology (Figure 6) and elongated cell
601 morphology (i.e., filamentation), particularly in stationary phase (Figures 7-8). Lack of DksA
602 also dramatically reduced bacterial culturability upon extended incubation in depleted broth
603 (Figure 9). Given the link to the stringent response, the Δ*dksA* strain may be physiologically
604 poorly equipped to handle nutrient deprivation or other stressors found in depleted broth.
605 Biologically, PsrA does not contribute to this phenotype. RNA-Seq analyses of Δ*psrA* or *in trans*
606 *psrA* expression strains showed few stress-related genes under PsrA regulation (Graham *et al*.,

607 2021), so PsrA may be dispensable in these conditions. Further to this, filamentation and
608 culturability likely influence DksA-dependent variability in optical density to titre ratios of
609 stationary phase bacteria recovered from three-day old BCYE plates, and thus explain the
610 variability in the *in vitro* growth curves, and potentially, the low inoculum titre in the *in vivo*
611 kinetics. Indeed, DksA was recently ascertained to have a pivotal role in cell division in *E. coli*;
612 binding of ppGpp to DksA/RNAP indirectly activates the divisome complex component FtsZ to
613 modulate cell length and division (Anderson *et al*., 2023). The absence of either DksA or ppGpp
614 promotes cell filamentation for different reasons; lack of DksA prevents activation of cell
615 division by ppGpp resulting whereas lack of ppGpp causes DksA to switch from an activator to
616 an inhibitor of FtsZ. Thus, by orthologous function, it is likely that DksA behaves in the same
617 manner in *L. pneumophila* as Δ*dksA* cells are filamentous (Figures 7 and 8) (Dalebroux *et al.,*
618 2010b). Lastly, pigmentation comprises a brown tyrosine-based metabolite produced post-
619 exponentially by *L. pneumophila* as an adaptation to environmental stress, potentially serving for
620 photoprotection, iron acquisition, or as a biocide to enhance *L. pneumophila* competitiveness in
621 biofilms (Steinert *et al.,* 1995; Chatfield and Cianciotto, 2017; Levin *et al.,* 2019). As reported
622 elsewhere, DksA is a major driver of pigment production (Figure 10) (Dalebroux *et al.,* 2010b).
623 Conversely, these traits, other than cell length, do not seem measurably impacted by the cellular
624 levels of PsrA, indicating that PsrA may impact virulence specific pathways rather than cellular
625 physiology.

626 Fatty acid flux is linked to *L. pneumophila* TP differentiation through SpoT-mediated
627 stringent induction, with either DksA or ppGpp, sufficient to arrest growth upon supplementation
628 with SCFA (Edwards *et al.,* 2009; Dalebroux *et al.,* 2010b). Here, we show that like its ortholog
629 in *Pseudomonas* spp., PsrA is responsive to fatty acids suggesting a conserved functional role in

630 sensing LCFA in the environment alongside SpoT, and further, both DksA and PsrA must be
631 present to ensure a proper LCFA response (Figure 11) (Kang *et al.*, 2008), although the
632 mechanistic details of the PsrA-mediated response remain undefined until further study can be
633 undertaken.

634 Together, our findings show that the truncation in DksA1 affects different biological
635 processes in different ways, with phenotypes of *dksA1* strains ranging from identical to the
636 parental strain, to identical to that of the full Δ*dksA* mutant, or intermediate to either, illustrating
637 that the dysfunctional DksA1 may impact different cellular processes in different ways given the
638 wide disparities in phenotypes attributed to this allele. As the functional basis of the *dksA1*
639 phenotype has not been elucidated, these results cannot distinguish the distinct effects of ppGpp
640 recruitment and competitive sequestration of RNAP from GreA; the presence of multiple DksA-
641 mediated regulatory mechanisms could contribute to the variability of phenotypes observed in
642 hypomorphic strains. Nevertheless, the fortuitous *dksA1* mutation allowed the opportunity to
643 further explore the regulatory dynamics between DksA and PsrA. The bacterial response to
644 LCFA suggests a novel regulatory link to the stringent response pathway, further solidifying the
645 mechanistic importance of both DksA and PsrA as contributing regulators of the biphasic
646 lifestyle of *L. pneumophila.*

647 In summary, PsrA seems to redundantly act as a bypass for *dksA* in virulence but has
648 little impact on other processes, suggesting a more targeted mechanism. The largely overlapping
649 and additive phenotypes presented in this study are consistent with the two distinct mechanisms
650 by which DksA and PsrA act, and thus the following model is proposed (Figure 12). In a
651 scenario in which a promoter that is repressed by either DksA or PsrA; absence of DksA would
652 permit GreA to act as the sole-secondary channel binding protein thereby allowing increased

653 efficiency in transcription initiation. Elevated levels of PsrA would result in increased promoter
654 blockage at co-regulated promoters, thus providing a compensatory repression. Conversely, lack
655 of PsrA would leave the promoter more accessible for RNAP, but this could be counteracted if
656 elevated levels of DksA results in reduced transcriptional efficiency. Alternatively, a promoter
657 not subject to PsrA influence would be exempt from the compensatory effects, and thus be
658 wholly dependent on the dynamics between GreA and DksA. Nevertheless, the proposed co-
659 regulator duality could explain why transcriptomic analyses did not overtly reveal a large
660 number of PsrA-regulated targets (Graham *et al*., 2021); thus, future transcriptomic studies will
661 include the Δ*psrA* Δ*dksA* strain to compare against data obtained for individual Δ*psrA* and Δ*dksA*
662 strains to discern distinct and overlapping roles.

663 Another major question is whether the observations garnered from the Δ*dksA* strain can
664 be extended to include the $ppGpp^0$ (Δ*relA* Δ*spoT*) strain. The interface with PsrA and ppGpp
665 remains unexplored and bears interest in relation to the link between PsrA and the fatty acid
666 response. The possibility that PsrA is the mechanism by which DksA drives the LCFA response
667 in $ppGpp^0$ strain is intriguing. Additionally, whether a similar reciprocal compensatory effect on
668 phenotypes is seen between $ppGpp^0$ and PsrA poses an interesting topic for future investigation
669 to follow upon the present study, which explored the phenotypic role of spontaneously mutated
670 DksA1 and PsrA, and uncovered a synergistic genetic relationship between PsrA and DksA in
671 terms of virulence regulation.
672
673
674
675

Acknowledgements

We thank M. Swanson (University of Michigan) for her kind gift of pBH6119 and Lp02, J. Vogel (Washington University) for his kind gift of pSR47s and pJB908, R. R. Isberg (Tufts University) for his kind gift of Lp03. This work was supported by Natural Sciences and Engineering Research Council (NSERC) Discovery Grant funds awarded to A.K.C.B (RGPIN-2019-05490), T.dK. (RPIN-2017-04970) and G.P. (RGPIN-2018-04968), and Canadian Foundation for Innovation (CFI) Grant funds to A.K.C.B. Research personnel were supported by University of Manitoba Faculty of Graduate Studies (C.G., T.M, T.P., J.B.), Research Manitoba Master's Studentship Award (T.P.), and NSERC CGS Masters (T.M, A.G.) and Doctoral (T.M., T.P, A.G.).

Materials and methods

Structural Predictions and Modelling The amino acid sequences of DksA and DskA1 were submitted to the collabfold2 sever (Pettersen *et al*. 2021) with default settings. Top rank #1 models were selected for modelling and analysis in UCSF ChimeraX (Pettersen *et al*., 2021). Structural overlays between Lp02 DksA, DksA1, and DksA (5VSW) (Molodtsov *et al*., 2018) were aligned with Matchmaker. Conservation alignments were performed using Consurf (Landau *et al*., 2005; Ashkenazy *et al*., 2016) with the Alphafold2 model of Lp02 DksA.

Culture of *E. coli* and *L pneumophila* *Legionella pneumophila* Philadelphia-1 derivative Lp02 parental and isogenic strains, as described in Table 1, were grown as previously described on Buffered-Charcoal-Yeast Extract BCYE)-agar plates (Feeley *et al.*, 1979) supplemented as required with thymidine (100 µg/mL), sucrose (5% w/v) or kanamycin sulphate (25 µg/mL) and incubated at 37°C and 5% CO_2, or Buffered-Yeast Extract (BYE) broth at 37°C. *E. coli* was utilized for cloning and plasmid propagation purposes (DH5α for *in trans* expression vector pJB908 or pThy [pBH6119], and DH5α λpir for suicide vector pSR47S)was grown on LB (Lennox) agar or broth supplemented as required with ampicillin (100 µg/mL) or kanamycin sulphate (40 µg/mL) and incubated at 37°C.

Molecular methods/reagents, cloning, and sequencing Chemicals were procured form VWR (Ottawa, ON, Canada), Thermo-Fisher (Mississauga, ON, Canada), or Sigma-Aldrich (Oakville, ON, Canada) while restriction enzymes, PCR enzymes, and other cloning reagents were procured from New England Biolabs (Whitby, ON, Canada). Oligonucleotide primers, ordered from Life Technologies (Thermo-Fisher), were utilized under conditions listed in Table 2.

722 Nucleic acid purification kits were purchased from Qiagen (Toronto, ON, Canada). Sanger
723 sequencing for routine verification of constructs and mutant validations was done as a fee-based
724 service by The Centre for Applied Genomics (The Hospital for Sick Children, Toronto, ON,
725 Canada). Whole genome sequencing was undertaken by phenol-chloroform isolation of genomic
726 DNA followed by sequencing via Pacbio SMRT at Genome-Québec (Montreal, QC, Canada)
727 and assembled using Geneious™ software.
728 ***dskA1* and Δ*dksA* mutant strains** The *dksA1* mutation was identified during routine whole
729 genome sequencing of prospective Δ*psrA* mutant strains during experiments for Graham *et al.*
730 (2021), and traced back to the electrocompetent cell stock used to create the strains, which was
731 subsequently struck out for isolated colonies. Colonies were screened for *dksA1* by PCR using
732 the primer set (PF dksA1 missing / PR dksA1 missing) that annealed to the missing 24 bp region
733 within *dksA1*, allowing recovering of the ancestral Lp02 *dksA1* strain from the competent cells.
734 For these reactions, PF dksA1 missing was paired with PR dksA ext conf, and PF dksA ext conf
735 was paired with PR dksA1 missing, such that each primer set only generated product from the
736 parental allele. As a positive PCR control, adjacent PF/PR dksA conf int primer set generated
737 product in both alleles. For generation of an in-frame Δ*dksA* mutant strain, ~1000 bp 5′ (primer
738 set PF 5-flk dksA SalI / PR 5-flk dksA BamH1) and 3′ (PF 3-flk dksA BamH1 / PR 3-flk dksA
739 SacI) regions flanking *dksA* were PCR-amplified and cloned into suicide vector pSR47S to use
740 for routine allelic exchange. For generation of *in trans* complementation or overexpression
741 constructs, either *dksA* or *dksA1* were PCR-amplified from Lp02 or *dksA1* mutant CG799,
742 respectively, using primer set (PF comp dksA BamHI / PR comp dksA SacI) and cloned into
743 pJB908, and introduced into parental or isogenic mutant strains by electroporation. Plasmid
744 constructs and mutations were routinely verified by sequencing isolated plasmids or PCR

745 amplicon products, and mutant strains were routinely subjected to whole genome sequencing to
746 rule out secondary mutations.
747
748 ***In vitro* growth kinetics** *L. pneumophila* strains were streaked on BCYE and grown for three
749 days under standard conditions. Bacterial cell mass was collected with a disposable loop and
750 suspended in pre-warmed BYE broth and normalized to OD_{600} = 0.15 in BYE broth.
751 Subsequently 150 µL of this suspension was loaded in triplicate wells in a 96-well flat bottomed
752 microtitre plate, the lid was sealed with Parafilm, and loaded into a BioTek Synergy HTX plate
753 reader, reading OD_{600} hourly for 24 h at 37°C or every 2 h for 48 h at 25°C with 150 rpm linear
754 shaking. Results were plotted in GraphPad Prism™ 9.1 and analyzed via two-way ANOVA
755 analysis.
756
757 **Culture and intracellular kinetics in protozoan *A. castellanii*** *Acanthamoeba castellanii*
758 (ATCC 30234) were propagated in PYG media at 25°C as previously described (Tanner *et al.,*
759 2016). Briefly, infections were undertaken in AC buffer by placing ~10^6 protozoan trophozoites
760 in each well of a set of 24 tissue culture-treated 24-well plates and allowing them to adhere, then
761 overlaying them with bacteria normalized by OD_{600} to a MOI of 0.1 in AC buffer. After 1 h
762 incubation at 25°C, the wells were washed 3 x 1 mL AC buffer, before incubating in 1 mL/well
763 of AC buffer at 25°C until the indicated timepoints. Protozoa were lysed mechanically via
764 vortexing, and the lysate serially diluted in AC buffer onto BCYE-agar plates to enumerate titres.
765 To enhance enumeration of difficult-to-recover avirulent strains, a portion of the lysate was
766 tenfold concentrated by centrifugation at 21,000 x *g* in a microcentrifuge for 2 min, then 0.9 vol
767 of the supernatant drawn off; the pellet was resuspended in the remaining volume and spotted

768 alongside the serial dilutions. After counting titres, graphs were plotted and analyzed (two-way
769 ANOVA) in GraphPad Prism™ 9.1.
770
771 **Culture and intracellular kinetics in U937 human macrophages** Human U937 monocytic
772 cells were propagated and differentiated into macrophages using phorbol myristate acetate
773 (PMA, Sigma-Aldrich) as previously described (Tanner *et al.,* 2016). Cells were grown in
774 RPMI-1640 media (HyClone, Thermo-Fisher) supplemented with 10% heat inactivated fetal
775 bovine serum (Seradigm, Mississauga, ON) (RPMI + FBS) at 37°C and 5% CO_2 that was used
776 for all washes and incubations in a pre-warmed state. For infection, ~ 10^6 activated U937-derived
777 macrophages were placed into each well of a tissue culture-treated 24 well plates, allowed to
778 adhere, and overlaid with *L. pneumophila* strains normalized by OD_{600} to a MOI of 2, for 1 h.
779 The bacteria were washed away with 3 x 1 ml washes in RPMI + FBS, followed by an
780 incubation for 1 h with RPMI + FBS with 100 µg/mL gentamicin. After a further 3 x 1 mL
781 washes in RPMI + FBS, the cells were incubated in 1 mL RPMI + FBS until lysis at indicated
782 timepoints. Cells were lysed osmotically by replacing the RPMI + FBS with ice-cold HyClone
783 ultrapure water and repeated pipetting (Thermo-Fisher), then serially diluting the lysate in
784 additional HyClone water and enumerating *L. pneumophila* titres by spotting the dilutions on
785 BCYE-agar plates. After counting, graphs were plotted and analyzed via two-way ANOVA in
786 GraphPad Prism™ 9.1.
787
788 **Pigment, morphology and capturability assays** Suspensions of *L. pneumophila* were prepared
789 as per *in vitro* growth kinetics. Pigment assays were undertaken in accordance to Wiater et al.
790 (1994). Briefly, inoculated 5 mL BYE broth cultures in 13 mL plastic test tubes were placed on a

791 roller drum at 37°C for 72 h. To quantify pigment at 24 h timepoints, 1 mL of culture was
792 withdrawn, pelleted at 21,000 x g in a microcentrifuge for 2 min, after which 150 µL of
793 supernatant was loaded in triplicate into 96 well plates and read for absorbance at 550 nm on a
794 BioTek Synergy HTX plate reader (Wiater *et al*., 1994). After removal of residual supernatant,
795 the pellet was suspended in 1 mL of 1 x PBS pH 7.0 and similarly loaded (150 µL) into a 96 well
796 plate then read for OD_{600}. Blank controls were the same volume of BYE or 1 x PBS as
797 appropriate. Results were plotted and analyzed using GraphPad Prism™ (9.1). Photographed
798 samples were prepared similarly and at specified allowed to sit undisturbed for 24 h at ambient
799 temperatures (~22°C) for cells to sediment out by gravity. Long-term culturability was assessed
800 by inoculating 96 well plates with six wells for each strain, containing 150 µL of an OD_{600} =
801 0.15 suspension in BYE. The outermost rows and columns were filled with sterile water to
802 reduce evaporation, the plates were sealed with Parafilm and incubated on a shaking platform at
803 37°C for four days. At indicated intervals, cell aggregates were dispersed with pipetting, the
804 OD_{600} was read with a BioTek Synergy HTX plate reader across the wells containing
805 unharvested culture, and one well of each strain harvested and serially diluted for titre on BCYE
806 agar plates. Results were plotted and analyzed using GraphPad Prism (9.1). For colony-spot
807 morphology, 10 µL of the residual OD_{600} = 0.15 suspension used to prepare these assays was
808 spotted on a BCYE plate with spots spread out to twice the spacing of a standard multi-channel
809 pipette then incubated for 4 days at 37ºC and 5% CO_2, then photographed.
810
811 **LCFA assays** Suspensions of *L. pneumophila* strains were prepared as per the *in vitro* kinetics,
812 at OD_{600} = 0.15 in BYE broth, except that media was supplemented with two-fold serially diluted
813 concentrations of palmitic acid (PA) as a 40 mM stock dissolved in 100% ethanol. All broth

814 including PA dilutions, controls and blanks was normalized to 0.5% ethanol. The suspension was
815 then subject to a standard in vitro growth curve as described in the in vitro kinetics section.
816 Inhibition was defined as growth of <50% in comparison to that of the same strain in a BYE +
817 0.5% ethanol-only control at the end of 24 h. Data were graphed using GraphPad Prism™ 9.1.
818
819 **Microscopy** Microscopy and cell lengths were conducted as per Graham *et al.,* (2021). Briefly,
820 broth cultures in BYE broth were inoculated at OD_{600} = ~0.02 and incubated for 18 hto OD_{600} =
821 0.5-1.0 at 37°C to enter exponential phase, then were mounted on a 2% w/v agarose pad
822 prepared in water and imaged on an Axio Observer Z1 inverted microscope (Zeiss) equipped
823 with a glycerol-immersion 150X objective. Stationary phase cells were imaged by returning the
824 cultures to the roller drum for a further ~24 h to achieve stationary phase and imaged similarly.
825 Cell lengths were quantified using the length tool in ImageJ and lengths plotted and analyzed in
826 GraphPad Prism™ (9.1).
827
828
829
830
831
832
833
834
835
836

837 **Table 1** List of strains and plasmids

Number	Name	Description	Source/reference
E. coli			
	DH5α	F′ *endA1 hsdR17*(r_k- m_k-) *supE44 thi-1 recA1 gyrA* (*Nal*^{r}) *relA1* Δ(*lacZYA-argF*)*U169 deoR*(ϕ80lacΔ(lacZ)M15)	New England Biolabs
	DH5α λpir	K-12 F- φ80*lacZ*ΔM15 *endA recAhsdR17* (*rm-mK*+) *supE44 thi-1 gyrA96 relA1* Δ(*lacZYA-argF*) U169 *λpir*	M. Swanson (Bryan *et al*., 2013)
L. pneumophila			
C858	Lp02	Str^r, Thy$^-$, HsdR$^-$ derivative of Philadelphia-1 strain	M. Swanson (Berger and Isberg, 1993)
KB265	Lp03	Lp02 Δ*dotA* mutant	R. Isberg (Berger and Isberg, 1993)
CG859	Δ*psrA*	Lp02 Δ*psrA* (unmarked, in frame deletion mutant)	Graham *et al.,* (2021)
CG860	Lp02 pThy	Lp02 pBH6119	Tanner *et al*., (2016)
JT708	Δ*dotA* pThy	Lp03 pBH6119	Tanner *et al*., (2016)
CG861	Lp02 pComp-*psrA*	Lp02 pJB908-*psrA*	Graham *et al.,* (2021)
CG862	Δ*psrA pThy*	Δ*psrA* pThy	Graham *et al.,* (2021)
CG863	Δ*psrA* pComp-*psrA*	Δ*psrA* pJB908-*psrA*	Graham *et al.,* (2021)
CG799	*dksA1*	Lp02 *dksA1* (*dksA1*[Δ*170-194]*); spontaneous 24 bp in-frame deletion	This study
CG819	*dksA1* pThy	*dksA1* pBH6119	This study
CG813	*dksA1*Δ*psrA*	Lp02 *dksA1* Δ*psrA*	This study
CG826	*dksA1* Δ*psrA* pThy	*dksA1* Δ*psrA* pBH6119	This study
CG1053	Δ*dksA*	Lp02 Δ*dksA* (unmarked, in frame deletion mutant of *dksA*)	This study
CG1054	Δ*dksA* Δ*psrA*	Δ*psrA* Δ*dksA*	This study
CG1055	Δ*dksA* pThy	Δ*dksA* pBH6119	This study
CG1056	Δ*dksA* Δ*psrA* pThy	Δ*psrA* Δ*dksA* pBH6119	This study
CG1057	Δ*dksA* pComp-*dksA*	Δ*dksA* pBH6119	This study
CG1059	Lp02 pComp-*dksA*	Lp02 pJB908-*dksA*	This study
CG1060	Δ*psrA* pComp-*dksA*	Δ*psrA* pJB908-*dksA*	This study
CG1061	Δ*dksA* pComp-*psrA*	Δ*dksA* pJB908-*psrA*	This study
CG1101	Δ*dksA* pComp-*dksA1*	Δ*dksA* pJB908-*dksA1*	This study
CG1102	Lp02 pComp-*dksA1*	Lp02 pComp-*dksA1*	This study
CG1146	*dksA1* pComp-*dksA*	*dksA1* pComp-*dksA*	This study
Plasmids			
	pJB908	RSF1010 cloning vector, *td*Δ*i*, Amp^r Thy$^+$	J. Vogel (Sexton *et al*., 2004)
	pBH6119	RSF1010 promoterless GFP vector; Amp^r, Thy$^+$	M. Swanson (Hammer *et al*., 2002)
	pSR47S	oriTRP4 oriR6K *kan*^{r} *sacB*	J. Vogel (Merriam *et al*., 1997)
pPP619	pComp-*psrA*	pJB908-*psrA*	Graham *et al.,* (2021)

pCG1051	pComp-*dksA*	pJB908-*dksA*	This study
pCG1080	pComp-*dksA1*	pJB908-*dksA1* allele recovered from spontaneous *dksA1* Lp02 strain CG799	This study
pCG1069	pSR47S-5′flk-*ΔdksA*-3′flk	pSR47S with 5′ and 3′ flanking regions for Δ*dksA*	This study

838

839

840

841 **Table 2** List of oligonucleotides.

Name	Sequence	Annealing Temp. (ºC)	Product Size (bp)
Cloning/Confirmation			
PF 5-flk dksA SalI	gcgataGTCGACgttagaggcagaacttttactctg	62	915
PR 5-flk dksA BamH1	gcgataGGATCCatcaattaattgtcctgtcatgcc		
PF 3-flk dksA BamH1	gcgataGGATCCcagggtgcttgattctttcttg	62	978
PR 3-flk dksA SacI	gcgataGAGCTCgtaataagggctctgtagtgagg		
PF comp dksA BamHI	gcgataGGATCCgatttcagcaaagaggcattgg	62	1016 (*dksA*) 992 (*dksA1*)
PR comp dksA SacI	gcgataGAGCTCgaatcaagcaccctgattttgg		
PF dksA ext conf	caagcaatcggaataacaaacc	62	842
PR dksA ext conf	cactgtaagccttgttgattttc		
PR dksA conf int	gtcttgcttcaagacgtttcag	57.5	533 (with PF ext dksA conf)
pF dksA1 missing*	ggaagaagtagatcgtactgtctc	57.5	320 with pF ext dksA conf*
PR dksA1 missing*	gagacagtacgatctacttcttcc	57.5	546 to pR ext dksA conf*
Sequencing			
PF pSR47s seq	ctgttgcatgggcataaagttg	-	–
PR pSR47s seq	cacaggaaacagctatgacc	-	-
PF pJB908 seq	ctccgtgatggaatgacaac	-	–
PR pJB908 seq	gaccgcttctgcgttctga	-	–

842 Restriction sites indicated by capitalized letters.

843 * dksA1 missing primers used for screening strains, anneal to the region missing in *dksA1* and
844 will only generate product with the parental allele.

845

846

847

848

849

850

851

852 **References**

853 1. Abdelhady, H. and Garduño, R.A. (2013) The progeny of *Legionella pneumophila* in human
854 macrophages shows unique developmental traits. *FEMS Microbiol Lett*. **349**:99-107.
855 2. Aberg, A., Shingler, V. and Balsalobre, C. (2008) Regulation of the *fimB* promoter: a case
856 of differential regulation by ppGpp and DksA *in vivo*. *Mol Microbiol*. **67**:1223-1241.
857 3. Aberg, A., Fernández-Vázquez, J., Cabrer-Panes, J.D., Sánchez, A. and Balsalobre, C.
858 (2009). Similar and divergent effects of ppGpp and DksA deficiencies on transcription in
859 *Escherichia coli. J Bacteriol.* **191**: 3226-3236.
860 4. Abu-Zant, A., Asare, R., Graham, J.E. and Abu Kwaik, Y. (2006. Role for RpoS but not
861 RelA of *Legionella pneumophila* in modulation of phagosome biogenesis and adaptation to
862 the phagosomal microenvironment. *Infect Immun.* **74**:3021-3026.
863 5. Al-Khodor, S., Kalachikov, S., Morozova, I., Price, C. T. and Abu Kwaik, Y. (2009) The
864 PmrA/PmrB two-component system of *Legionella pneumophila* is a global regulator
865 required for intracellular replication within macrophages and protozoa. *Infect Immun*.
866 **77**:374-386.
867 6. Anderson, S.E., Vadia, S.E., McKelvy, J. and Levin, P.A. (2023) The transcription factor
868 DksA exerts opposing effects on cell division depending on the presence of ppGpp. *mBio*
869 14(6):e0242523.
870 7. Ashkenazy, H., Abadi, S., Martz, E., Chay, O., Mayrose, I., Pupko, T. and Ben-Tal, N.
871 (2016) ConSurf 2016: an improved methodology to estimate and visualize evolutionary
872 conservation in macromolecules. *Nucleic Acids Res* 8;44(W1):W344-50.
873 8. Bachman, M.A. and Swanson**,** M.S. (2001) RpoS co-operates with other factors to induce
874 *Legionella pneumophila* virulence in the stationary phase. *Mol Microbiol.* **40**:1201-1214.

875 9. Burstein, D., Amaro, F., Zusman, T., Lifshitz, Z., Cohen, O., Gilbert, J.A., Pupko, T.,
876 Shuman, H.A. and Segal, G. (2016) Genomic analysis of 38 *Legionella* species identifies
877 large and diverse effector repertoires. *Nat Genet.* **48**:167-175.
878 10. Chatfield, C.H. and Cianciotto, N.P. (2007). The secreted pyomelanin pigment of *Legionella*
879 *pneumophila* confers ferric reductase activity. *Infect Immun*. **75**: 4062-4070.
880 11. Chatterji, D., Fujita, N. and Ishihama, A. (1998) The mediator for stringent control, ppGpp,
881 binds to the beta-subunit of *Escherichia coli* RNA polymerase. *Genes Cells* **3**:279-287.
882 12. Dalebroux, Z.D., Svensson, S.L., Gaynor, E.C. and Swanson, M.S. (2010a) ppGpp conjures
883 bacterial virulence. *Microbiol Mol Biol Rev.* **74**:171-199.
884 13. Dalebroux, Z.D., Yagi, B.F., Sahr, T., Buchrieser, C. and Swanson, M.S. (2010b) Distinct
885 roles of ppGpp and DksA in *Legionella pneumophila* differentiation. *Mol Microbiol.* **6**:200-
886 219.
887 14. Edwards, R.L., Dalebroux, Z.D. and Swanson, M.S. (2009) *Legionella pneumophila* couples
888 fatty acid flux to microbial differentiation and virulence. *Mol Microbiol.* **71**:1190-1204.
889 15. Faulkner, G. and Garduño, R.A. (2002) Ultrastructural analysis of differentiation in
890 *Legionella pneumophila. J Bacteriol.* **184**:7025-7041.
891 16. Feldheim Y.S., Zusman T., Speiser Y. and Segal G. (2016) The *Legionella pneumophila*
892 CpxRA two-component regulatory system: new insights into CpxR's function as a dual
893 regulator and its connection to the effectors regulatory network. *Mol Microbiol.* **99**:1059-
894 1079.
895 17. Finsel, I. and Hilbi, H. (2015) Formation of a pathogen vacuole according to *Legionella*
896 *pneumophila*: how to kill one bird with many stones. *Cell Microbiol*. **17**:935-950.

897 18. Fonseca, M.V. and Swanson, M.S. (2014) Nutrient salvaging and metabolism by the
898 intracellular pathogen *Legionella pneumophila*. *Front Cell Infect Microbiol.* **4**:12.
899 19. Garduño, R.A., Garduño, E., Hiltz, M. and Hoffman, P.S. (2002) Intracellular growth of
900 *Legionella pneumophila* gives rise to a differentiated form dissimilar to stationary-phase
901 forms. *Infect Immun.* **70**:6273-6283.
902 20. Gomez-Valero, L., Rusniok, C., Carson, D., Mondino, S., Pérez-Cobas, A.E., Rolando, M.,
903 Pasricha, S., Reuter, S., Demirtas, J., Crumbach, J., Descorps-Declere, S., Hartland, E.L.,
904 Jarraud, S., Dougan, G., Schroeder, G.N., Frankel, G. and Buchrieser, C. (2019b) More than
905 18,000 effectors in the *Legionella* genus genome provide multiple, independent
906 combinations for replication in human cells. *Proc Natl Acad Sci U S A.* **116**:2265-2273.
907 21. Gourse, R.L., Chen, A.Y., Gopalkrishnan, S., Sanchez-Vazquez, P., Myers, A. and Ross, W.
908 (2018) Transcriptional Responses to ppGpp and DksA. *Annu Rev Microbiol.* **72**:163-184.
909 22. Graham, C.I., Patel, P.G., Tanner, J.R., Hellinga, J., MacMartin, T.L., Hausner, G. and
910 Brassinga, A.K.C. (2021) Autorepressor PsrA is required for optimal *Legionella*
911 *pneumophila* growth in *Acanthamoeba castellanii* protozoa. *Mol Microbiol*. **116**:624-647.
912 23. Graham, C.I., MacMartin, T.L., de Kievit, T.R. and Brassinga, A.K.C. (2024) Molecular
913 regulation of virulence in *Legionella pneumophila*. *Mol Microbiol*. **121**:167-195.
914 24. Gummesson, B., Lovmar, M. and Nyström, T. (2013) A proximal promoter element
915 required for positive transcriptional control by guanosine tetraphosphate and DksA protein
916 during the stringent response. *J Biol Chem.* **288**:21055–21064.
917 25. Hales, L.M. and Shuman, H.A. (1999) The *Legionella pneumophila rpoS* gene is required
918 for growth *within Acanthamoeba castellanii*. *J Bacteriol.* **181**:4879-4889.

919 26. Hammer, B.K., Tateda, E.S. and Swanson, M.S. (2002) A two-component regulator induces
920 the transmission phenotype of stationary-phase *Legionella pneumophila. Mol Microbiol.*
921 **44**:107-118.
922 27. Häuslein, I., Sahr, T., Escoll, P., Klausner, N., Eisenreich, W. and Buchrieser, C. (2017)
923 *Legionella pneumophila* CsrA regulates a metabolic switch from amino acid to glycerolipid
924 metabolism. *Open Biology* **7**:170149.
925 28. Hovel-Miner, G., Pampou, S., Faucher, S.P., Clarke, M., Morozova, I., Morozov, P., Russo,
926 J.J., Shuman, H.A. and Kalachikov, S. (2009) SigmaS controls multiple pathways associated
927 with intracellular multiplication of *Legionella pneumophila. J Bacteriol.* **191**:2461-2473.
928 29. Isberg, R.R., O'Connor, T.J. and Heidtman, M. (2009) The *Legionella pneumophila*
929 replication vacuole: making a cozy niche inside host cells. *Nat Rev Microbiol.* **7**:13-24.
930 30. Jumper, J., Evans, R., Pritzel, A., Green, T., Figurnov, M., Ronneberger, O.,
931 Tunyasuvunakool, K., Bates, R., Žídek, A., Potapenko, A., Bridgland, A., Meyer, C., Kohl,
932 S.A.A., Ballard, A.J., Cowie, A., Romera-Paredes, B., Nikolov, S., Jain, R., Adler, J., Back,
933 T., Petersen, S., Reiman, D., Clancy, E., Zielinski, M., Steinegger, M., Pacholska, M.,
934 Berghammer, T., Bodenstein, S., Silver, D., Vinyals, O., Senior, A.W., Kavukcuoglu, K.,
935 Kohli, P. and Hassabis, D. (2021) Highly accurate protein structure prediction with
936 AlphaFold. *Nature* 596(7873):583-589.
937 31. Kagan, J.C. and Roy, C.R. (2002) *Legionella* phagosomes intercept vesicular traffic from
938 endoplasmic reticulum exit sites. *Nat Cell Biol.* **4**:945-954.
939 32. Kang, Y., Nguyen, D.T., Son, M.S. and Hoang, T.T. (2008) The *Pseudomonas aeruginosa*
940 PsrA responds to long-chain fatty acid signals to regulate the *fadBA5* beta-oxidation operon.
941 *Microbiology* **154**:1584-1598.

942 33. Landau, M., Mayrose, I., Rosenberg, Y., Glaser, F., Martz, E., Pupko, T. and Ben-Tal, N.
943 (2005) ConSurf 2005: the projection of evolutionary conservation scores of residues on
944 protein structures. *Nucleic Acids* Res 33(Web Server issue):W299-302.
945 34. Lemke, J.J., Sanchez-Vazquez, P., Burgos, H.L., Hedberg, G., Ross, W. and Gourse, R.L.
946 Direct regulation of *Escherichia coli* ribosomal protein promoters by the transcription
947 factors ppGpp and DksA. *Proc Natl Acad Sci USA.* 108(14):5712-7.
948 35. Levin, T.C., Goldspiel, B.P., Malik, H.S. (2019). Density-dependent resistance protects
949 *Legionella pneumophila* from its own antimicrobial metabolite, HGA. *Elife.* **8**: e46086.
950 36. McNealy, T.L., Forsbach-Birk, V., Shi, C. and Marre, R. (2005) The Hfq homolog in
951 *Legionella pneumophila* demonstrates regulation by LetA and RpoS and interacts with the
952 global regulator CsrA. *J Bacteriol.* **187**:1527-1532.
953 37. Magnusson, L.U., Gummesson, B., Joksimović, P., Farewell, A. and Nyström, T. (2007)
954 Identical, independent, and opposing roles of ppGpp and DksA in *Escherichia coli. J*
955 *Bacteriol.* **189**:5193-5202.
956 38. Molodtsov, V., Sineva, E., Zhang, L., Huang, X., Cashel, M., Ades, S.E. and Murakami,
957 K.S. (2018) Allosteric Effector ppGpp Potentiates the Inhibition of Transcript Initiation by
958 DksA. *Mol Cell* 69(5):828-839.e5.
959 39. Molofsky, A.B. and Swanson, M.S. (2004) Differentiate to thrive: lessons from the
960 *Legionella pneumophila* life cycle. *Mol Microbiol.* **53**:29-40.
961 40. Mondino, S., Schmidt, S. and Buchrieser, C. (2020) Molecular mimicry: a paradigm of host-
962 microbe coevolution illustrated by *Legionella*. *mBio* **11**:e01201-20.
963 41. Morash, M.G., Brassinga, A.K., Warthan, M., Gourabathini, P., Garduño, R.A., Goodman,
964 S.D. and Hoffman, P.S. (2009) Reciprocal expression of integration host factor and HU in

965 the developmental cycle and infectivity of *Legionella pneumophila*. *Appl Environ*
966 *Microbiol.* **75**:1826-1837.
967 42. Myers, A.R., Thistle, D.P., Ross, W. and Gourse, R.L. (2020) Guanosine Tetraphosphate
968 Has a Similar Affinity for Each of Its Two Binding Sites on *Escherichia coli* RNA
969 Polymerase. *Front Microbiol* 11:587098.
970 43. Nevo, O., Zusman, T., Rasis, M., Lifshitz, Z. and Segal, G. (2014) Identification of
971 *Legionella pneumophila* effectors regulated by the LetAS-RsmYZ-CsrA regulatory cascade,
972 many of which modulate vesicular trafficking. *J Bacteriol.* **196**:681-692.
973 44. Newton, H.J., Ang, D.K., van Driel, I.R. and Hartland, E.L. (2010) Molecular pathogenesis
974 of infections caused by *Legionella pneumophila. Clin Microbiol Rev.* **23**:274-298.
975 45. Oliva, G., Sahr, T. and Buchrieser, C. (2018) The life cycle of *L. pneumophila*: cellular
976 differentiation is linked to virulence and metabolism. *Front Cell Infect Microbiol.* **8**:3.
977 46. Parshin, A., Shiver, A.L., Lee, J., Ozerova, M., Schneidman-Duhovny, D., Gross, C.A. and
978 Borukhov, S. (2015) DksA regulates RNA polymerase in *Escherichia coli* through a
979 network of interactions in the secondary channel that includes Sequence Insertion 1. *Proc*
980 *Natl Acad Sci U S A* 112(50):E6862-71.
981 47. Perederina, A., Svetlov, A., Vassylyeva, M., Tahirov, T., Yokoyama, S., Artsimovitch, I.
982 and Vassylyev, D. (2004). Regulation through the secondary channel-structural framework
983 for ppGpp-DksA synergism during transcription. *Cell* **118**:297-309.
984 48. Personnic, N., Striednig, B. and Hilbi, H. (2018) *Legionella* quorum sensing and its role in
985 pathogen-host interactions. *Curr Opin Microbiol.* **41**:29-35.

986 49. Pettersen, E.F., Goddard, T.D., Huang, C.C., Meng, E.C., Couch, G.S., Croll, T.I., Morris,
987 J.H. and Ferrin, T.E. (2021) UCSF ChimeraX: Structure visualization for researchers,
988 educators, and developers. *Protein Sci.* 30(1):70-82.
989 50. Pitre, C.A.J., Tanner, J.R., Patel, P. and Brassinga, A.K.C. (2013) Regulatory control of
990 temporally expressed integration host factor (IHF) in *Legionella pneumophila. Microbiology*
991 **159**:475-492.
992 51. Potrykus, K. and Cashel, M. (2008) (p)ppGpp: still magical? *Annu Rev Microbiol*. **62**:35-51.
993 52. Rasis, M. and Segal, G. (2009) The LetA-RsmYZ-CsrA regulatory cascade, together with
994 RpoS and PmrA, post-transcriptionally regulates stationary phase activation of *Legionella*
995 *pneumophila* Icm/Dot effectors. *Mol Microbiol.* **72**:995-1010.
996 53. Robertson, P., Abdelhady, H. and Garduño, R.A. (2014) The many forms of a pleomorphic
997 bacterial pathogen-the developmental network of *Legionella pneumophila*. *Front Microbiol*.
998 **5**:670.
999 54. Ross, W., Vrentas, C.E., Sanchez-Vazquez, P., Gaal, T. and Gourse, R.L. (2013) The magic
1000 spot: a ppGpp binding site on *E. coli* RNA polymerase responsible for regulation of
1001 transcription initiation. *Mol Cell* 50(3):420-9.
1002 55. Ross, W., Sanchez-Vazquez, P., Chen, A.Y., Lee, J.H., Burgos, H.L. and Gourse, R.L.
1003 (2016) ppGpp Binding to a Site at the RNAP-DksA Interface Accounts for Its Dramatic
1004 Effects on Transcription Initiation during the Stringent Response. *Mol Cell* 62(6):811-823.
1005 56. Rowbotham, T.J. (1986) Current views on the relationships between amoebae, legionellae
1006 and man. *Isr J Med Sci*. **22**:678-689.

1007 57. Sahr, T., Bruggemann, H., Jules, M., Lomma, M., Albert-Weissenberger, C., Cazalet, C. and
1008 Buchrieser, C. (2009) Two small ncRNAs jointly govern virulence and transmission in
1009 *Legionella pneumophila. Mol Microbiol.* **72**:741-762.
1010 58. Sahr, T., Rusniok, C., Dervins-Ravault, D. Sismeiro, O., Coppée, J.Y. and Buchrieser, C.
1011 (2012) Deep sequencing defines the transcriptional map of L. pneumophila and identifies
1012 growth phase-dependent regulated ncRNAs implicated in virulence. *RNA Biol*. **9**:503-19.
1013 59. Sahr, T., Rusniok, C., Impens, F., Oliva, G., Sismeiro, O., Coppée, J.Y. and Buchrieser, C.
1014 (2017) The *Legionella pneumophila* genome evolved to accommodate multiple regulatory
1015 mechanisms controlled by the CsrA-system. *PLoS Genet.* **13**:e1006629.
1016 60. Schell, U., Kessler, A. and Hilbi, H. (2014) Phosphorylation signalling through the
1017 *Legionella* quorum sensing histidine kinases LqsS and LqsT converges on the response
1018 regulator LqsR. *Mol Microbiol.* **92**:1039-1055.
1019 61. Skolnick, J., Gao, M., Zhou, H. and Singh, S. (2021) AlphaFold 2: Why It Works and Its
1020 Implications for Understanding the Relationships of Protein Sequence, Structure, and
1021 Function. *J Chem Inf Model* 61(10):4827-4831.
1022 62. Steinert, M., Engelhard, H., Flugel, M., Wintermeyer, E. and Hacker J. (1995). The Lly
1023 protein protects *Legionella pneumophila* from light but does not directly influence its
1024 intracellular survival in *Hartmannella vermiformis*. *Appl Environ Microbiol.* **61**: 2428-2430.
1025 63. Steinert, M., Hentschel, U. and Hacker, J. (2002) *Legionella pneumophila*: an aquatic
1026 microbe goes astray. *FEMS Microbiol Rev*. **26**:149-162.
1027 64. Tanner, J.R., Li, L., Faucher, S.P. and Brassinga, A.K. (2016) The CpxRA two-component
1028 system contributes to *Legionella pneumophila* virulence. *Mol Microbiol.* **100**:1017-1038.

1029 65. Tanner, J.R., Patel, P.G., Hellinga, J.R., Donald, L.J., Jimenez, C., LeBlanc, J.J. and
1030 Brassinga, A.K.C. (2017) *Legionella pneumophila* OxyR Is a redundant transcriptional
1031 regulator that contributes to expression control of the two-component CpxRA system. *J*
1032 *Bacteriol.* **199**:e00690-16.
1033 66. Tiaden, A., Spirig, T., Weber, S.S., Brüggemann, H., Bosshard, R., Buchrieser, C. and Hilbi,
1034 H. (2007) The *Legionella pneumophila* response regulator LqsR promotes host cell
1035 interactions as an element of the virulence regulatory network controlled by RpoS and LetA.
1036 *Cell Microbiol.* **9**:2903-2920.
1037 67. Tiaden, A., Spirig, T., Carranza, P., Brüggemann, H., Riedel, K., Eberl, L., Buchrieser, C.
1038 and Hilbi, H. (2008) Synergistic contribution of the *Legionella pneumophila lqs* genes to
1039 pathogen-host interactions. *J Bacteriol.* **190**:7532-7547.
1040 68. Tilney, L.G., Harb, O.S., Connelly, P.S., Robinson, C.G. and Roy, C.R. (2001) How the
1041 parasitic bacterium *Legionella pneumophila* modifies its phagosome and transforms it into
1042 rough ER: implications for conversion of plasma membrane to the ER membrane. *J Cell Sci.*
1043 **114**:4637-4650.
1044 69. Vinella, D., Potrykus, K., Murphy, H. and Cashel, M. (2012) Effects on growth by changes
1045 of the balance between GreA, GreB, and DksA suggest mutual competition and functional
1046 redundancy in *Escherichia coli. J Bacteriol.* **194**:261–273.
1047 70. Wiater, L.A., Sadosky, A.B. and Shuman, H.A. (1994) Mutagenesis of *Legionella*
1048 *pneumophila* using Tn*903* dll*lacZ*: identification of a growth-phase-regulated pigmentation
1049 gene. *Mol Microbiol*. **11**:641-653.

1050 71. Zusman, T., Gal-Mor, O. and Segal, G. (2002) Characterization of a *Legionella*
1051 *pneumophila relA* insertion mutant and toles of RelA and RpoS in virulence gene
1052 expression. *J Bacteriol.* **184**:67-75.
1053 72. Zusman, T., Aloni, G., Halperin, E., Kotzer, H., Degtyar, E., Feldman, M., Segal, G. (2007)
1054 The response regulator PmrA is a major regulator of the *icm/dot* Type IV secretion system
1055 in *Legionella pneumophila* and *Coxiella burnetii*. *Mol Microbiol.* **63**:1508-1523.

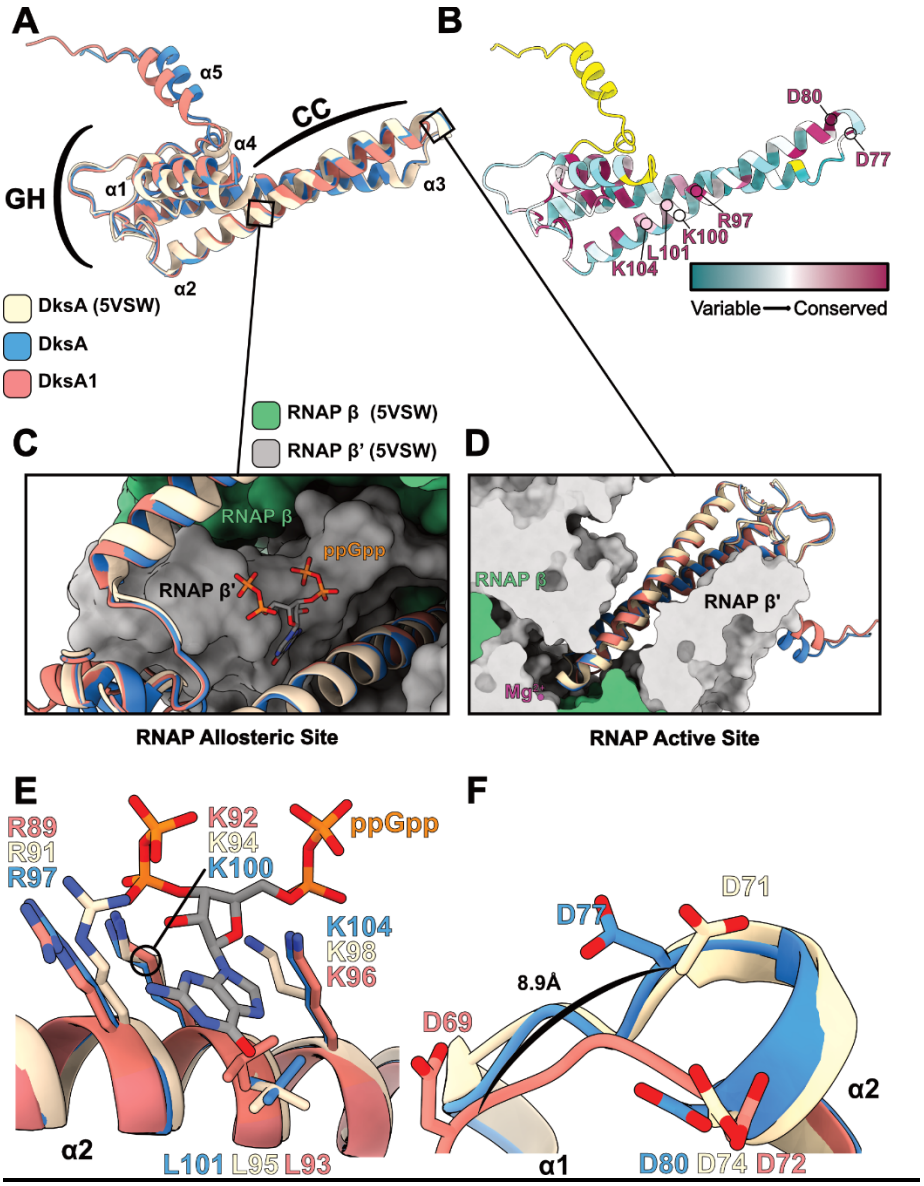

Figure 1: Structural comparison of DksA and DksA1 AlphaFold models. (A) Structural overlay of DksA (PDB ID: 5VSW) with both Lp02 DksA and DksA1 as modeled by AlphaFold. (B) Residue conservation of Lp02 DskA as plotted by the server Consurf (Landau *et al*., 2005; Ashkenazy *et al*., 2016). Yellow indicates insufficient information in the multisequence alignment. Indicated on the structure are conserved residues important for binding ppGpp and allostery with RNAP (R97 to K104), in addition to contact with the active site (D77-D80). (C) Binding of DksA with the RNAP allosteric site. A DksA:RNAP experimental structure (PDB ID: 5VSW) and aligned AlphaFold models are shown as cartoons, whereas RNAP is drawn as a molecular surface. The structure of ppGpp bound in the complex is also shown. (D) Slice view of DksA showing the contact point of residues D80 and D77 with magnesium in the RNAP active site. (D) Interactions of DksA variants with ppGpp in the RNAP allosteric site are shown and not disturbed by the truncation in DksA1. (E) Interactions of DksA variants with magnesium in the active site of RNAP are shown. AlphaFold predicts the truncation in DksA1 drastically moves the position of a critical aspartate residue (D69/71/77).

Figure 2

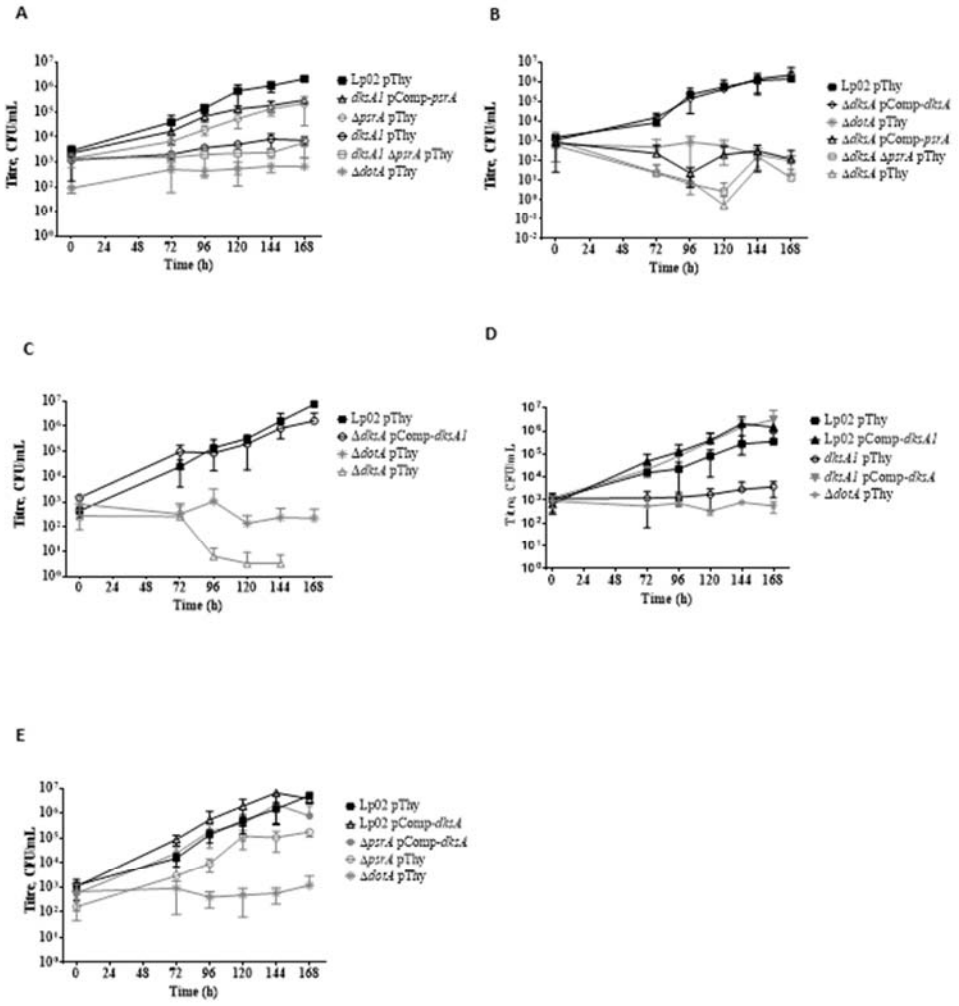

Figure 2: Synergistic impacts of DksA, DksA1, and PsrA on virulence of *L. pneumophila* in the *A. castellanii* protozoa. Intracellular growth kinetics of *L. pneumophila* strains in *A. castellanii* protozoa at 25ºC. Strains tested were parental Lp02 and isogenic strains featuring single or combinatorial genetics mutations (Δ*psrA*, Δ*dksA*, *dksA1*), *in-trans* complementation or overexpression of *psrA, dksA* or *dksA1* genes. Lp02 and Δ*dotA* are virulent (parental) and avirulent strains, respectively. Complementation/overexpression was via *in trans* plasmid expression with gene and endogenous promoter cloned into pJB908. pThy is empty control vector pBH6119. Error bars represent SD across mean of three biological replicates, with two technical replicates each. Samples below detection limit (~10 CFU/mL) were recorded as zero and omitted from graph if they lacked countable colonies across all replicates.

Figure 3

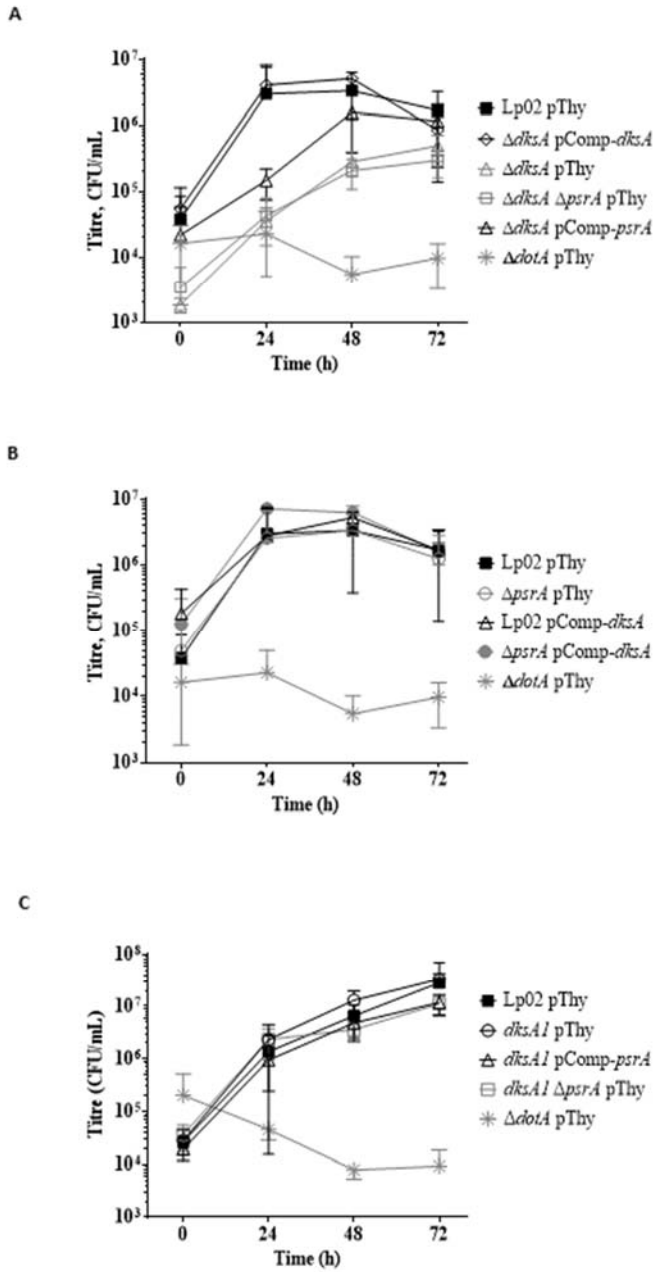

Figure 3: DksA is dispensable for growth in human macrophages. Intracellular growth kinetics of *L. pneumophila* strains in U937-derived macrophages at 37°C. Strains tested were parental Lp02 and isogenic strains featuring single or combinatorial genetic mutations (Δ*psrA*, Δ*dksA*, *dksA1*), *in-trans* complementation or overexpression of *psrA, dksA* or *dksA1* with gene and endogenous promoter cloned into pJB908. Lp02 and Δ*dotA* are virulent (parental) and avirulent strains, respectively. pThy is empty control vector pBH6119. Error bars represent SD across mean of three biological experiments with two technical replicates each. Experiments in panels A and B were conducted concurrently, but presented separately for clarity.

Figure 4

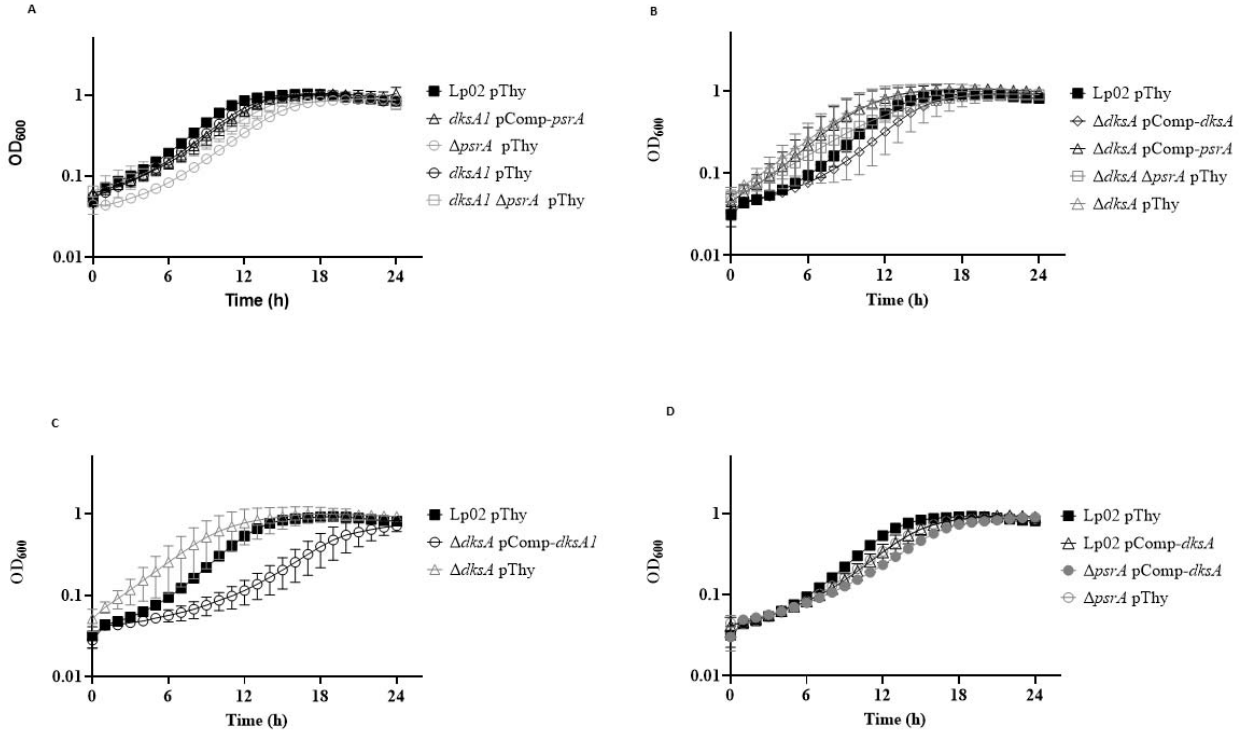

Figure 4: *L. pneumophila in vitro* growth at 37°C is impacted by DksA, PsrA and DksA1. *In vitro* growth kinetics of *L. pneumophila* strains: parental Lp02 and isogenic strains featuring single or combinatorial genetic mutations (Δ*psrA*, Δ*dksA*, *dksA1*) and/or *in-trans* complementation or overexpression of *psrA, dksA*, or *dksA1* genes. Plate-grown bacteria were suspended in BYE broth and normalized to initial OD_{600} = 0.15, and growth at 37°C was monitored for OD_{600} hourly for 24 h. Complementation/overexpression was via *in trans* plasmid expression with gene and endogenous promoter cloned into pJB908, pThy is empty control vector pBH6119. Graphs in panels A-D were experiments conducted concurrently, but presented separately for clarity. Error bars are SD across mean of three independent biological replicates with three technical replicates each.

Figure 5

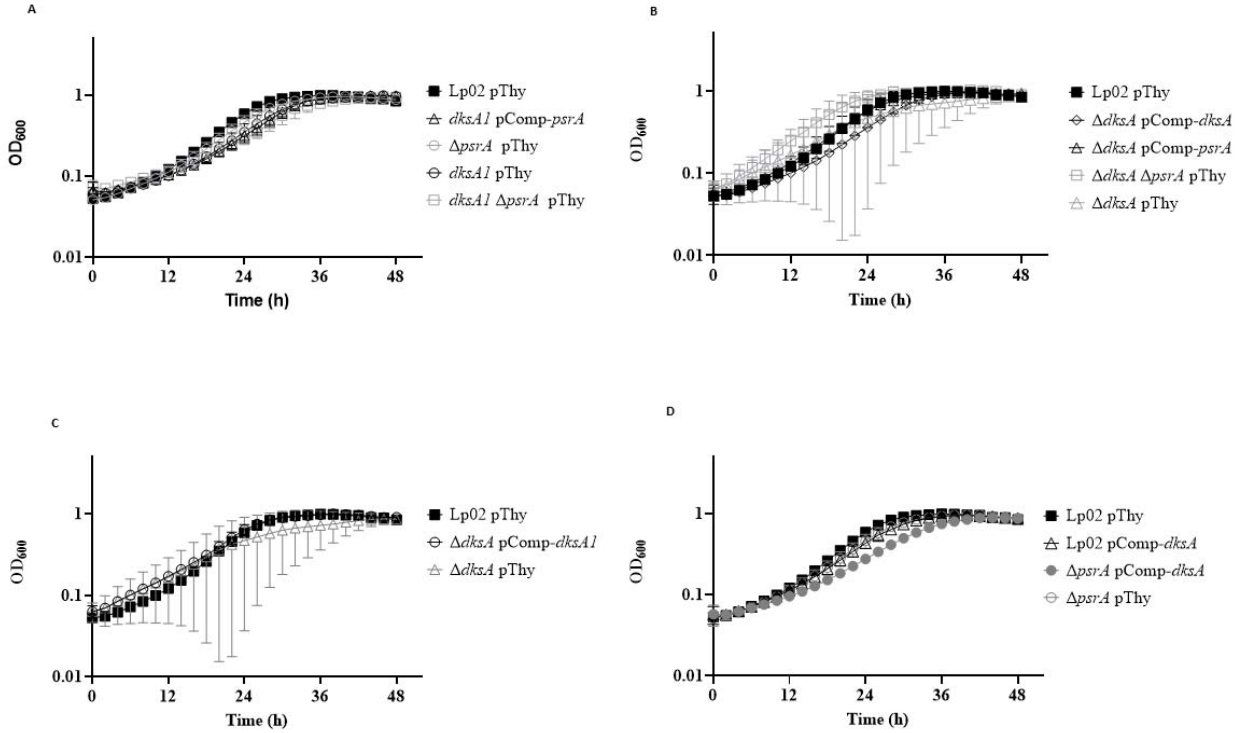

Figure 5: *L. pneumophila in vitro* growth at 25°C is impacted by DksA, PsrA and DksA1. *In vitro* growth kinetics of *L. pneumophila* strains: Parental Lp02 and isogenic strains featuring single or combinatorial genetic mutations (Δ*psrA*, Δ*dksA*, *dksA1*), *in-trans* complementation or overexpression of *psrA, dksA* or *dksA1* genes. Lp02 is the parental strain. Complementation/overexpression was via *in trans* plasmid expression with gene and endogenous promoter cloned into pJB908. pThy is empty control vector pBH6119. Plate-grown bacteria were re-suspended in BYE broth and normalized to initial OD_{600} = 0.15, and growth at 25°C was monitored for OD_{600} every 2 h for 48 h. Graphs in panels A-D were experiments conducted concurrently, but presented separately for clarity. Error bars are SD across mean of three independent biological replicates with three technical replicates each.

Figure 6

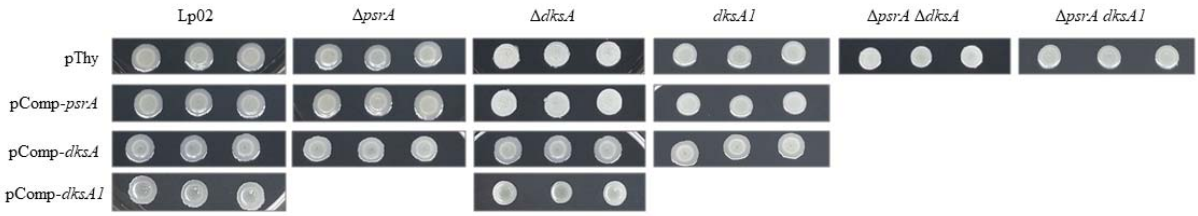

1113

1114 **Figure 6: *L. pneumophila* DksA and DksA1, but not PsrA affects colony morphology.**
1115 Parental Lp02 and isogenic strains featuring single or combinatorial genetic mutations (Δ*psrA*,
1116 Δ*dksA*, *dksA1*), and/or *in-trans* complementation or overexpression of *psrA* or *dksA* genes with
1117 gene and endogenous promoter cloned into pJB908. pThy is empty control vector pBH6119.
1118 Strains were grown on BCYE plates for 3 days and used to generate a bacterial suspension in
1119 BYE at OD_{600} = 0.15. 10 µL of the suspension was spotted onto BCYE plates in triplicate then
1120 the plates were incubated at 37°C at 5% CO_2 for 4 days prior to being photographed. Images are
1121 representative of one of three biological replicates.

Figure 7

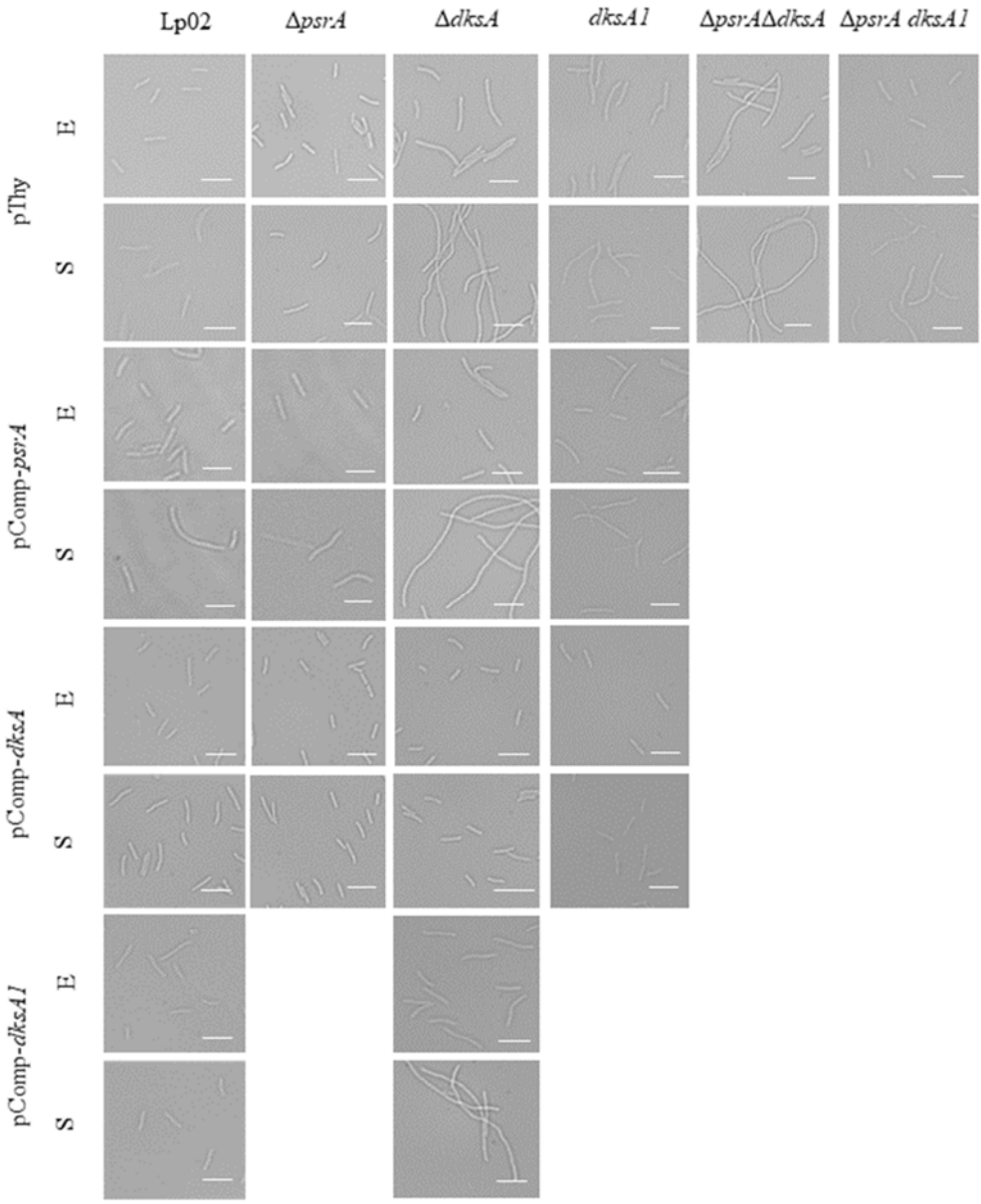

1122

1123 **Figures 7*: L. pneumophila* Δ*dksA*, but not *dksA1* or *psrA* cause filamentation.** Parental Lp02
1124 and isogenic strains featuring single or combinatorial genetic mutations (Δ*psrA*, Δ*dksA*, *dksA1*),
1125 *in-trans* complementation or overexpression of pComp-*psrA,* pComp-*dksA* or pComp-*dksA1*
1126 genes were grown on BCYE plates and used to inoculate a dilute suspension of OD_{600} = 0.02 in
1127 BYE broth then incubated overnight at 37°C with aeration, to exponential (E) (~18h , OD_{600} =
1128 ~0.5) or stationary (S; 24 h after EP) growth phases, then live-mounted on a 2% agarose pad
1129 prepared in ddH_2O and imaged on an Axio Observer Z1 inverted microscope (Zeiss) equipped
1130 with a glycerol-immersion 150X objective. Representative microscopic images of bacteria from
1131 one of three biological replicates. Scale bar is 5 µm.

Figure 8

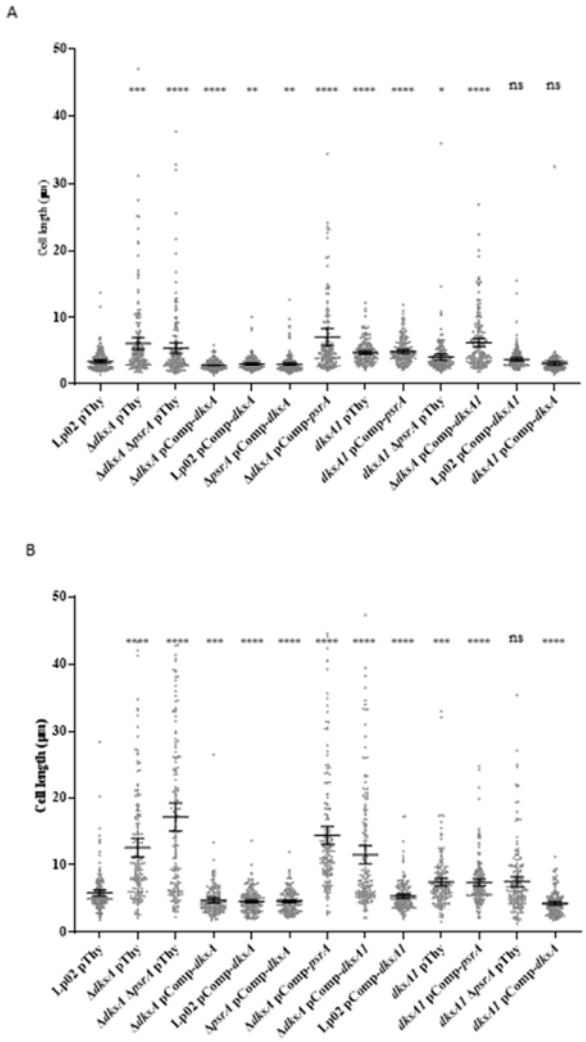

Figure 8*: L. pneumophila* Δ*dksA*, *dksA1*, and *psrA* contribute to cell length regulation. Parental Lp02 and isogenic strains featuring single or combinatorial genetic mutations (Δ*psrA*, Δ*dksA*, *dksA1*), *in-trans* complementation or overexpression of *psrA, dksA* or *dksA1* genes were grown from 3-day old plates subcultured to BYE broth at OD_{600} = 0.02 then incubated at 37°C with aeration to (A) exponential (overnight, OD_{600} ~ 0.5) or (B) stationary phases (24 h after exponential phase) then imaged with an Axio Observer Z1 inverted microscope (Zeiss) equipped with a glycerol-immersion 150X objective and individual bacterial cell lengths quantified using the length tool in ImageJ. Where filamentation was evident, only individual cells for which the full length was visible were measured. Data represents >150 individual readings spread equally across three biological replicates. Bar on graph and error bars represents mean and 95% confidence interval, respectively. Statistical significance determined by Student's T-test (*, $p < 0.05$; ** $p < 0.01$; *** $p < 0.001$; **** $p < 0,0001$; ns, not significant, $p > 0.05$).

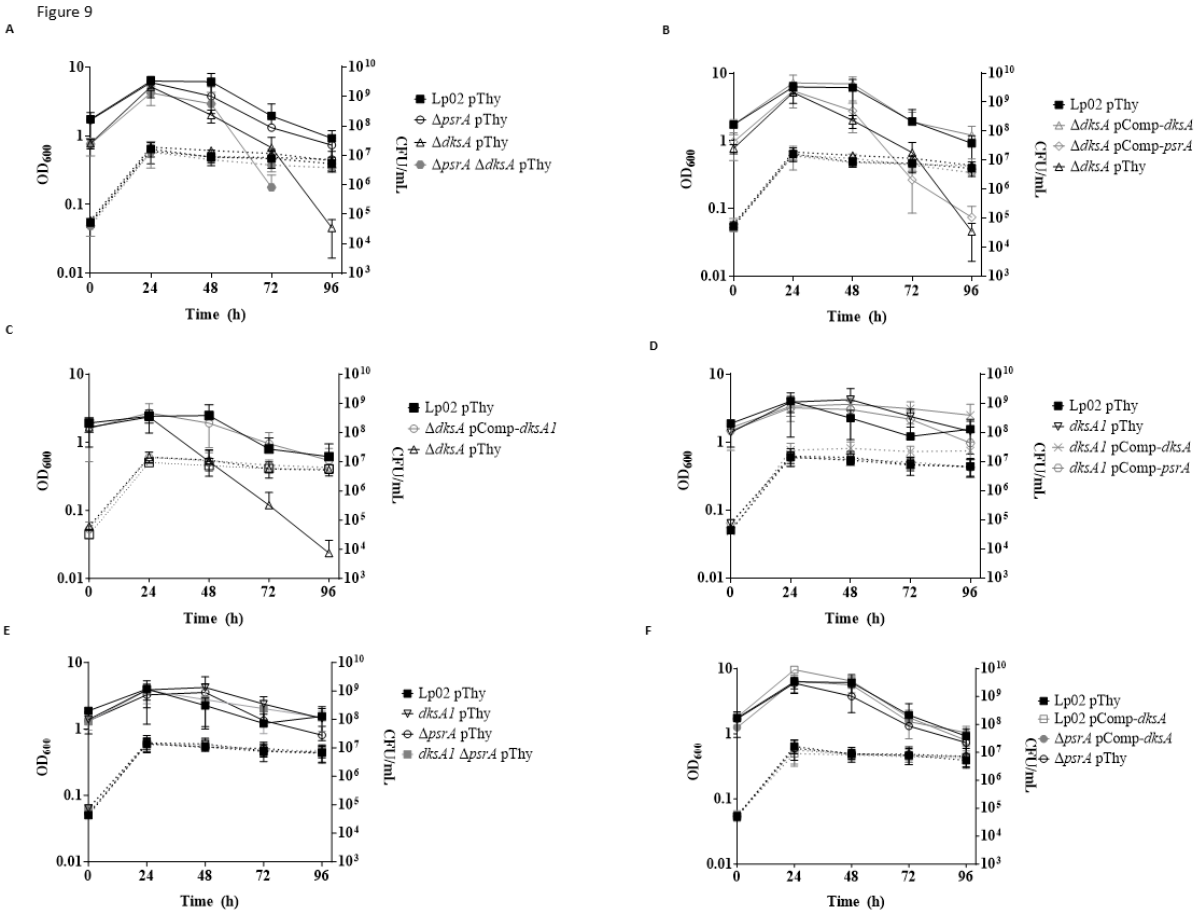

1145

1146 **Figure 9: Bacterial culturability in depleted nutrient media is dependent on DksA or**
1147 **DksA1, but not PsrA.** Panels (A-F) show *in vitro* growth kinetics of Lp02 and isogenic strains
1148 featuring single or combinatorial genetic mutations (Δ*psrA*, Δ*dksA*, *dksA1*), *in-trans*
1149 complementation or overexpression of *psrA, dksA* or *dksA1* genes, in BYE broth at 37°C for 96
1150 hours with OD_{600} values (dotted lines; left Y axis) and titre enumerated by serial dilution and
1151 incubation on BCYE plates (solid lines; right Y axis) at 24 h intervals. Data are presented as
1152 mean and SD of three biological replicates. Points were omitted if results could not be calculated
1153 (no colonies recovered, below detection limit of ~100 CFU/mL). For ease of comparison, data
1154 obtained for select strains (Lp02 pThy, Δ*psrA* pThy, Δ*dksA* pThy, *dksA1* pThy) are shown in
1155 more than one panel where panels represent data acquired concurrently.

Figure 10

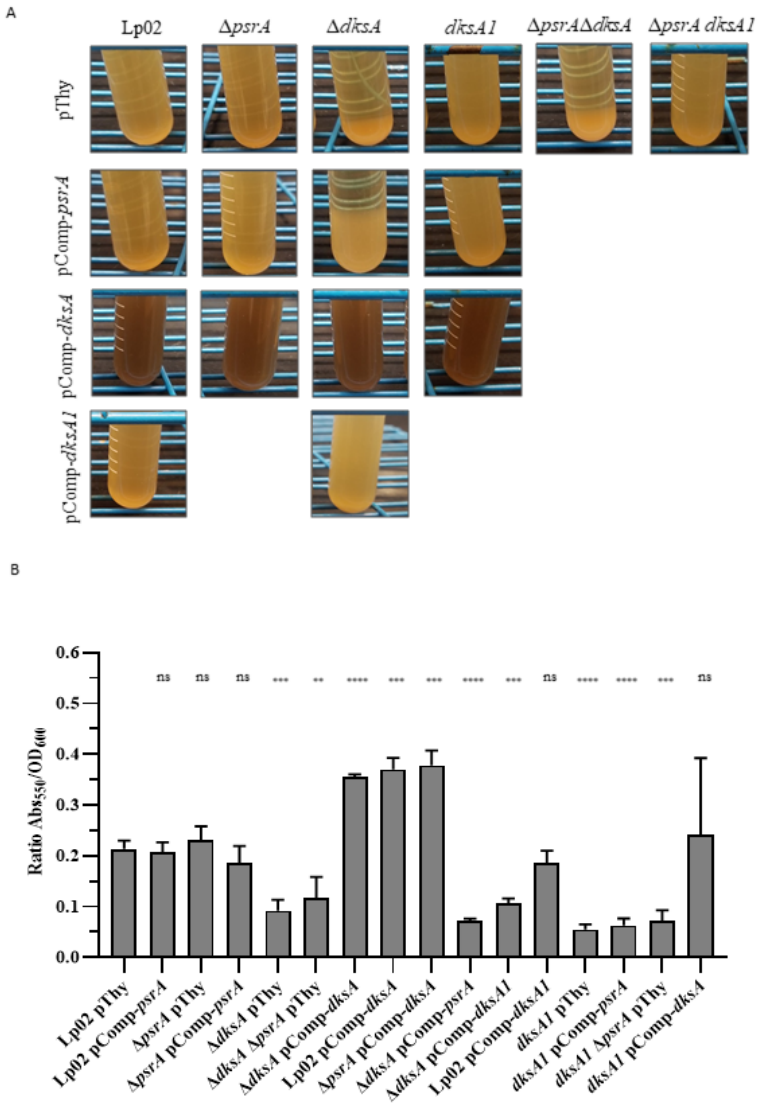

Figure 10: Pigmentation is regulated by DksA, but not PsrA. Parental Lp02 and isogenic strains featuring single or combinatorial genetic mutations (Δ*psrA*, Δ*dksA*, *dksA1*) and/or *in-trans* complementation or overexpression of *psrA, dksA* or *dksA1* genes, were grown on BCYE plates for 3 days and used to generate a 5 mL bacterial suspension (BYE at $OD_{600} = 0.15$) then incubated at 37°C for 30 h (a) Qualitative observation of pigmentation. After 48 h incubation tubes were set aside for 24 h at room temperature to allow cells to sediment out, then photographed. Representative image of three replicates. (b) Quantification of pigment at 30 h. After 30 h of incubation 1 mL of culture was centrifuged at 20,000 x *g*. The supernatant was measured for pigment levels via absorbance at 550 nm, then the pellet was resuspended in same volume of 1X PBS pH 7.0 to measure cell density via OD_{600}. Readings were taken with a plate reader in a 96 well plate relative to appropriate BYE or PBS blanks. Readings reflect Abs_{550} /OD_{600}. Error bars represent SD across three biological replicates. Statistical significance calculated via Student's T-Test and relative to parental Lp02 pThy, indicated above bars (*, $p < 0.05$, ** $p < 0.01$; *** $p < 0.001$; **** $p < 0{,}0001$; ns, not significant, $p > 0.05$).

Figure 11

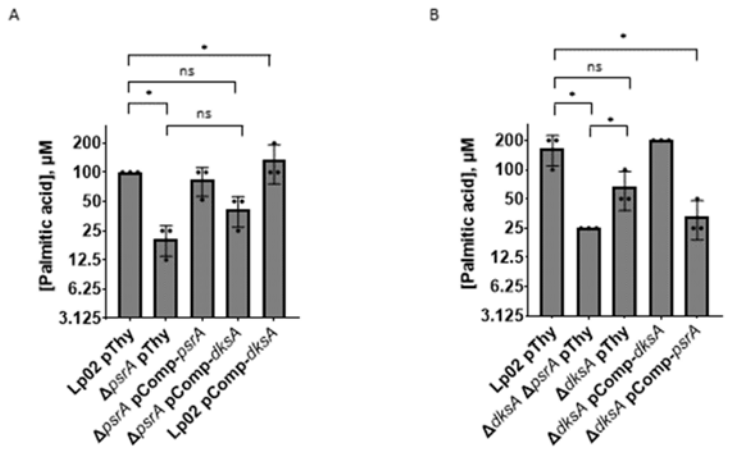

Figure 11: PsrA and DksA influences LCFA-mediated growth inhibition. Parental Lp02 and isogenic strains featuring single or combinatorial genetic mutations (Δ*psrA* and/or Δ*dksA*), and *in-trans* complementation or overexpression of *psrA* or *dksA* genes, grown with and without palmitic acid supplementation (as 40 mM stock dissolved in ethanol) in BYE media normalized to 0.5% ethanol, in a 96-well microplate for 24 h with shaking at 37°C. Inhibition was defined as growth, as assessed by OD_{600} values, of <50% of that of same strain in a BYE + 0.5% ethanol-only control at the end of 24 h. Bars indicate mean of maximum concentration of PA where indicated strain grew >50% of maximum, over three biological replicates with standard deviation indicated. Dots in bars indicate individual replicate values. Panels A and B were conducted separately. Statistical analyses were done using Student's unpaired T test: ns = no significance, * = $p<0.05$.

Figure 12

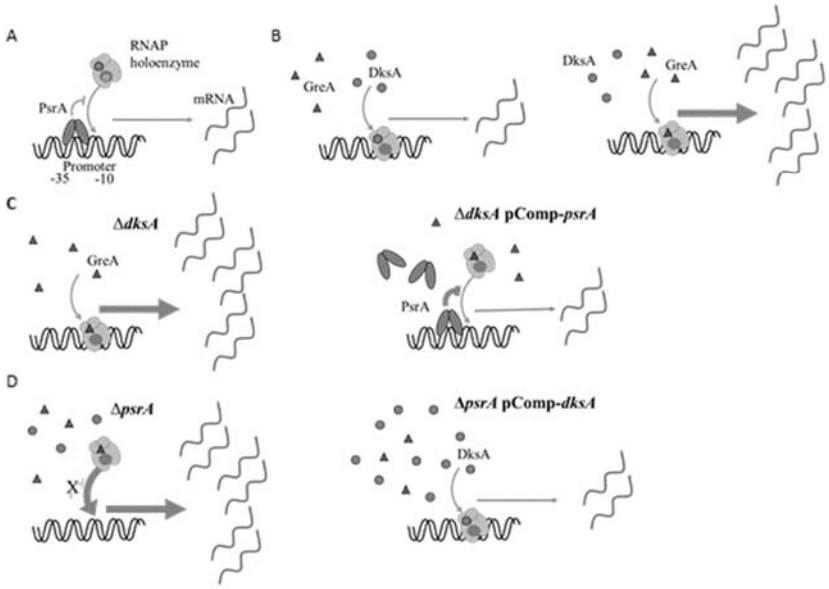

Figure 12: Model of independent mechanisms of DksA and PsrA. A hypothetical promoter is repressed by both PsrA and DksA (A) RNA polymerase (RNAP) holoenzyme is targeted to -10 and -35 boxes by a sigma factor. PsrA (oval dimers) binds a defined site in the promoter and inhibits RNAP recruitment. (B) RNAP binds to GreA (triangles) or DksA (filled octagons) interchangeably, with enhanced transcription initiation rates occurring while bound to GreA versus DksA. (C) In a Δ*dksA* strain, only GreA is available for RNAP thus elevating transcription levels, but *in trans psrA* overexpression generates higher levels of PsrA, strengthening inhibition of RNAP recruitment to compensate. Conversely (D) the Δ*psrA* strain allows uninhibited RNAP-promoter binding, increasing transcription, but this is offset by overexpressing *dksA in trans*, increasing the proportion of RNAP bound to transcription-inhibiting DksA thereby generating the compensatory effect.